Damping of Structures with Riveted Joints

A THESIS SUBMITTED IN PARTIAL FULFILLMENT
OF THE REQUIREMENTS FOR THE DEGREE OF

MASTER OF TECHNOLOGY
IN
MECHANICAL ENGINEERING

BY

SAHITYA DASARI
210ME2138

DEPARTMENT OF MECHANICAL ENGINEERING
NATIONAL INSTITUTE OF TECHNOLOGY
ROURKELA
2012

Damping of Structures with Riveted Joints

A THESIS SUBMITTED IN PARTIAL FULFILLMENT
OF THE REQUIREMENTS FOR THE DEGREE OF

MASTER OF TECHNOLOGY
IN
MECHANICAL ENGINEERING

BY

SAHITYA DASARI
210ME2138

Under the guidance of

Prof. B.K. NANDA

DEPARTMENT OF MECHANICAL ENGINEERING
NATIONAL INSTITUTE OF TECHNOLOGY
ROURKELA
2012

National Institute of Technology

Rourkela

Certificate

This is to certify that the thesis entitled, **"Damping of Structures with Riveted Joints"** submitted by Ms. Sahitya Dasari in partial fulfillment of the requirements for the award of *Master of Technology* degree in *Mechanical Engineering* with specialization in *Production Engineering* during session 2010-2012 at the National Institute of Technology, Rourkela.

It is an authentic work carried out by her under my supervision and guidance. To the best of my knowledge, the matter embodied in the thesis has not been submitted to any other University/Institute for the award of any degree or diploma.

Date:

Prof. B.K. Nanda
Dept. of Mechanical Engineering
National Institute of Technology

Acknowledgement

Successful completion of work will never be one man's task. It requires hard work in right direction. There are many who have helped to make my experience as a student a rewarding one. In particular, I express my gratitude to my thesis supervisor **Dr. B.K. Nanda, Professor, Department of Mechanical Engineering, NIT Rourkela** for kindly providing me to work under his supervision and guidance. I extend my deep sense of indebtedness and gratitude to him first for his valuable guidance, inspiring discussions, constant encouragement & kind co-operation throughout period of work which has been instrumental in the success of thesis.

I extend my thanks to **Dr. K.P. Maity, Professor and Head, Dept. of Mechanical Engineering, Department of Mechanical Engineering, NIT Rourkela** for extending all possible help in carrying out the dissertation work directly or indirectly.

I greatly appreciate and convey my heartfelt thanks to my friends, Praneeth Balasankula, Priyanka Jena, Ankita Singh, Abhishek Tiwari, Ashirbad Swain, dear ones & all those who helped me in completion of this work.

I feel pleased and privileged to fulfill my parent's ambition and I am greatly indebted to them for their moral support and continuous encouragement while carrying out this study. This thesis is dedicated to my family.

SAHITYA DASARI

Nomenclature

A	Area of cross-section of the beam
A_0	Area of cross-section of the rivet
A′	Area under a connecting rivet head
d	Diameter of connecting rivet
E	Static bending modulus of elasticity
E_f	Energy loss per cycle due to friction at joints
E_{loss}	Total energy loss per cycle
E_n	Energy stored in the system per cycle
E_0	Energy loss per cycle due to material and support friction
F_{rM}	Maximum frictional force at the interfaces
$2h_1$, $2h_2$	Thickness of each layer of the cantilever specimen
I	Second moment of area
k	Static bending stiffness of the layered and jointed beam
k′	Static bending stiffness of the solid beam
l	Length of individual elements
L	Free length of the layered and jointed beam
m	Number of layers in a jointed beam

N	Total normal force under each connecting rivet
p	Interface pressure
P	Preload on a rivet
q	Number of rivets
R	Any radius within influencing zone
R_B	Radius of the connecting rivet
R_M	Limiting radius of influencing zone
t	time coordinate
u_o	Relative dynamic slip between the interfaces at a riveted joint in the absence of friction
u_r	Relative dynamic slip between the interfaces at a riveted joint in the presence of friction
u_{rM}	Relative dynamic slip between the interfaces at the maximum amplitude of vibration
W	Static load
a_1,a_{n+1}	Amplitude of first cycle and last cycle, respectively
y(l, 0)	Initial free end displacement
n	Number of cycles

Greek Symbols

α	Dynamic slip ratio $(u_r/u_{o)}$
δ	Logarithmic decrement of the system
Δ	Deflection due to static load
μ	Kinematic coefficient of friction
ω_n	Natural frequency of vibration
ω_d	Damped frequency of vibration
ρ	Mass density
σ_o	Initial stress on a rivet
σ_s	Surface stress on the jointed structure
ξ	Damping ratio

Operators

‘.’	d/dt
‘,’	d/dx

Abstract

The main purpose of the structural design is to restrict the vibration of structures at a desirable level as per requirements. Usually, structures inherently possess low structural damping necessitating the introduction of additional measures to improve their damping characteristics in order to control the harmful effects of vibration in normal operating conditions. In fact, most monolithic structures possess low inherent damping thereby causing serious problems which will impair the function and life of structures leading to their ultimate failure. It is always desirable to keep the vibration level as low as possible by introducing damping so that the performance and useful life of structures are enhanced largely. Since many decades, it has been a biggest challenge to the practicing engineers and designers to limit this unwanted vibration in structures. In view of this, structures must be properly designed to possess adequate damping so that the undesirable vibration levels will not build-up beyond a permitted limit. The sole contribution of the present investigation is intended in this direction only. The design concept evolved from this research work of using layered structures with riveted joints can be effectively utilized in trusses and frames, aircraft and aerospace structures, bridges, machine members, robots and many other applications where higher damping is required.

The present investigation highlights the effect of interfacial slip on the damping of layered fixed beams jointed with rivets undergoing free vibration. The inclusion of mechanical joints bears a strong influence in the overall system performance and behavior, particularly the damping level of the structures. One of the techniques used in the present problem for improving damping is fabricating these structures in layers by means of riveted joints. The incorporation of such joints is the major source of energy dissipation through frictional effects associated with relative shear

displacements at the interfaces of the various structural members. Most of the damping in built-up structures is thus attributed to micro-slip at the interfaces. The contribution of the micro-slip on the overall system damping is always significant in spite of its low magnitude.

This thesis consists of two different parts: a theoretical analysis of the problem and an experimental work. The theoretical analysis proposes the classical method to calculate damping. The analyses are based on the assumptions of Euler-Bernoulli beam theory as the dimensions of test specimens satisfy the criterion of thin beam theory. A continuous model is characterized by a partial differential equation with respect to spatial and time coordinates. An analytical exact solution is obtained for the above differential equation from which the dynamic characteristics of the structure are represented accurately.

The logarithmic decrement technique has been used for measuring the damping from the time history curve of the decaying signals recorded on the screen of digital storage oscilloscope. The experimental results are compared with the corresponding theoretical ones. The damping characteristics in jointed structure are influenced by the intensity of pressure distribution, micro-slip and kinematic coefficient of friction at the interfaces the above vital parameters are largely influenced by the thickness ratio of the beam and thereby affect the damping capacity of the structures. Number of layers, fixed beam length and diameter of connecting rivet also play a key role on the damping capacity of the jointed structures quantitatively.

Table of Contents

List of Figures

List of Tables

Chapter 1

1 Introduction

The study of damping and its importance in structures has become increasingly significant for controlling the undesirable effects of vibration. Following the requirements of modern technology, there has been significant increase in demand to design, develop and fabricate machine tools, space structures, high speed automobiles, etc. to meet the global demand. The manufacture of such structures also requires high damping capacity and stiffness with light weight for its effective use. Such requirements demanded and popularized the use of welded, bolted and riveted layered beams as structural members with high damping capacity. In the alternative, cast structures can be used, but unfortunately, these are more expensive to manufacture and as a result, the deployment of welded, bolted and riveted multi-layered beam structures is becoming increasingly common in such industries. Joints have a great potential for reducing the vibration levels of a structure and have attracted the interest of many researchers. Many comprehensive review papers on joints and fasteners have appeared in recent years. Although a lot of work has been carried out on the damping capacity of bolted structures, but a little amount of work has been reported till date on the mechanism of damping in layered and jointed riveted structures. Furthermore, the effect of the aforesaid parameters on the damping rate of such structures is investigated and discussed in this study.

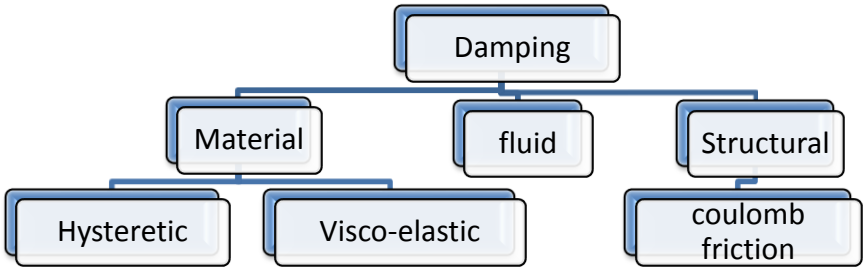

Figure 1: Hierarchy of damping

1.1 Damping

Damping is a phenomenon by which mechanical energy is dissipated (usually converted as thermal energy) in dynamic systems. It is the energy dissipation property of a material or system under cyclic stress. When a structure is subjected to an excitation by an external force then it vibrates in certain amplitude of vibration, it reduces as the external force is removed. This is due to some résistance offered to the structural member which may be internal or external. This resistance is termed as damping.

The study of damping has been taken up primarily in four major areas like Materials science, Structural mechanics, Vibration control and Inspection methods. The energy of the vibrating system is dissipated by various mechanisms and generally more than one mechanism may be present, concurrently. For convenience, damping in vibrating mechanical systems is classified depending on the main routes of energy dissipation as follows:

1. Material damping
2. Structural damping and
3. Fluid damping

1.1.1 Material damping of material

Coulomb postulated that material damping arises due to interfacial friction between the grain boundaries of the material under dynamic condition. When materials are critically stressed, energy is dissipated internally within the material itself. The internal or material damping is inherently low [1]. Hence, material damping is also known as solid or internal damping. It is

associated with the energy dissipation within the volume of material. This mechanism is usually related to internal restorations of the micro and macro structures ranging from crystal lattice to molecular scale effects, thermo-elasticity, grain boundary viscosity, point-defect relaxation, etc [2-3]. There are two types of internal damping:

1. Viscoelastic damping and
2. Hysteretic damping

1.1.1.1 Viscoelastic damping

Passive damping using viscoelastic materials (VEM's) is widely used in both commercial and aerospace applications. Viscoelastic materials are elastomeric materials whose long-chain molecules cause them to convert mechanical energy into heat when they are deformed. The relation between the stress and strain of a viscoelastic damping material is expressed through a linear differential equation with respect to time. The most widespread model used for viscoelastic damping is the Kelvin-Voigt model as it gives the most accurate results for practical purposes [4]. The stress-strain relationship given by this model is $\sigma = E\varepsilon + E^* \frac{d\varepsilon}{dt}$, where E and E^* are the Young's modulus and complex modulus of the material, respectively. The term $E\varepsilon$ represents the elastic behavior of the material with no contribution to damping, while the second term $E^* \frac{d\varepsilon}{dt}$ is responsible for damping. The damping capacity per unit volume is expressed as $d_v = E * \oint \frac{d\varepsilon}{dt} d\mathcal{E}$.

1.1.1.2 Hysteretic damping

Experiments by several investigators indicate that for most structural systems, the energy dissipated per cycle is independent of the frequency and approximately proportional to the stiffness of the system and square of amplitude of vibration. The energy loss per cycle is expressed as $E= \pi\ k\ \lambda\ A^2$, where k, λ and A are the stiffness of the system, dimensionless damping factor depending on the property of the material and amplitude of vibration, respectively. When a body having material damping is subjected to vibration, the stress-strain diagram shows a hysteresis loop whose area denotes the energy lost per cycle due to damping.

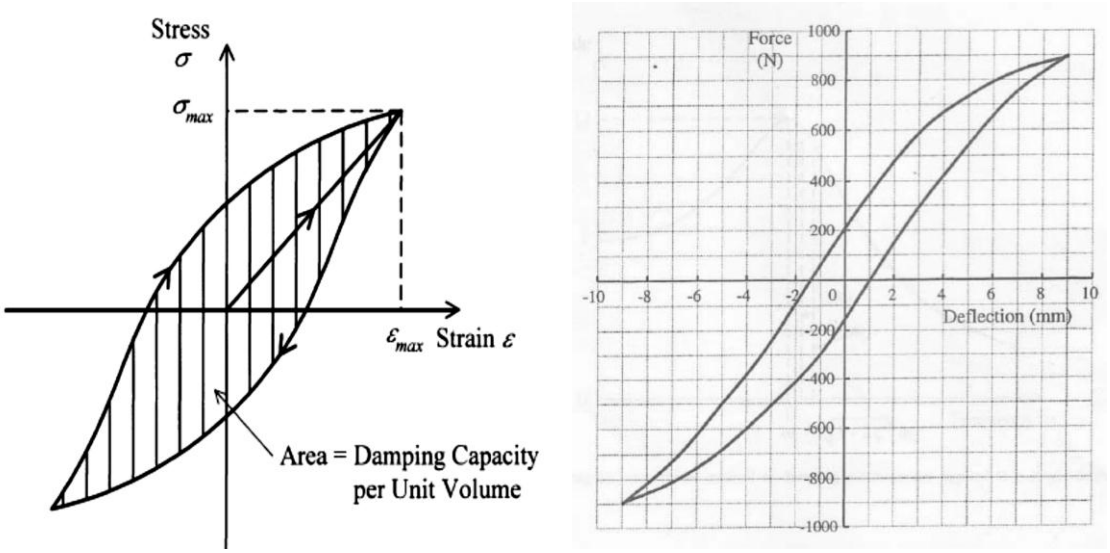

Figure 2: A typical hysteresis loop for material damping

The stress (σ) and strain (ε) relations at a point in a vibrating body possess a hysteresis loop as shown in Fig. 1. The area of the hysteresis loop gives the energy dissipation per unit volume of the material per stress cycle [4-5]. This is termed as specific damping capacity (Ψ) and given by the cyclic integral $\psi=\oint \sigma\, d\mathcal{E}$

1.1.2 Structural damping:

Since the damping in the structural material is not significant, most of the damping in real fabricated structures arises in the joints and interfaces [4,6]. It is the result of energy dissipation caused by rubbing friction resulting from relative motion between components and by intermittent contact at the joints in a mechanical system. However, the energy dissipation mechanism in a joint is a complex phenomenon being largely influenced by the interface pressure and degree of slip at the interfaces. System damping arises from slip and other boundary shear effects at mating surfaces, interfaces or joints between distinguishable parts. It is this slip phenomenon occurring in the presence of friction at the joint interface that causes the energy dissipation and nonlinearity in the joints. System damping involves configuration of distinguishable part arises from slip and boundary shear effects of mating surfaces. Energy dissipation during cyclic stress at an interface may occur as a result of dry sliding (coulomb friction), lubricated sliding (viscous forces) or cyclic strain in a separating adhesive (damping in visco-elastic layers between mating surfaces).

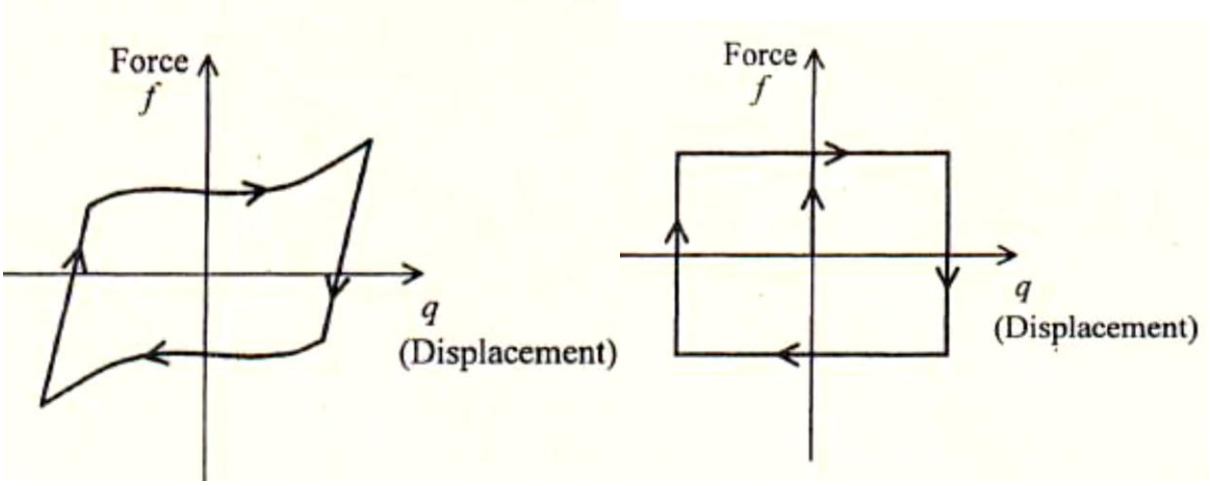

Figure 3: Representative hysteresis loops for Structural damping and Coulomb friction

1.1.3 Fluid damping - through fluid structure interactions:

There is a drag, resulting in the local displacement of the element relative to the surrounding fluid. This resistance is the cause of mechanical-energy dissipation in fluid damping.

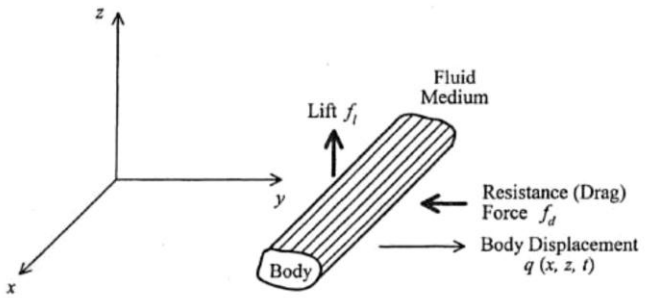

Figure 4: A body moving in a fluid medium

Appreciable structural damping has been achieved using layered and jointed structures with welded, riveted and bolted constructions. Joints are present in most of the structures and usually over ninety percent of the inherent damping in a fabricated structure originates in the joints. Hence, we are considering the riveted constructions for this study. The energy dissipated at the support is very small when compared to material damping [6]. As the material damping within the structural members is of low magnitude, various other techniques are used to improve the damping capacity of structures. These are:

1. Use of constrained/unconstrained viscoelastic layers, use of a viscous fluid layer,
2. Fabrication using a multi-layered sandwich construction,
3. Use of stress raisers, insertion of special high-elasticity inserts in the parent structure,
4. Application of spaced damping techniques,
5. Fabricating layered and jointed structures with welded/riveted/bolted joints.

1.2 Riveted Joints

A rivet is a short cylindrical bar with a head integral with it. The set head is made before hand on the body of the rivet by upsetting. The second, called the closing head, is formed during riveting. A riveted joint is made by inserting rivets into holes in the elements to be connected. A joint holding two or more elements together by the use of rivets is called riveted joints.

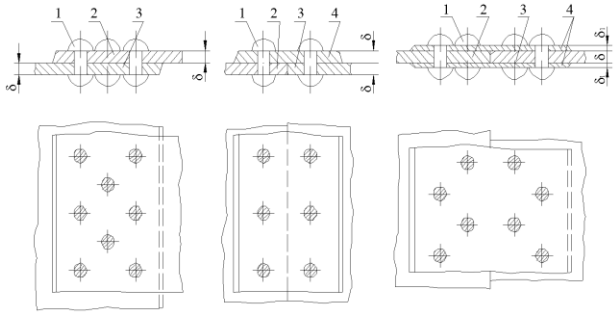

Figure 5: The ordinary forms of rivets after riveting

Rivets have been mostly standardized. They are usually made from steel, copper and aluminum. In recent years, titanium is also used as the material from which rivet is made.

Loads: Under ordinary conditions, the main loads acting on riveted joints are due to longitudinal forces that tend to shift one component of the joint relative to the other.

Failures: If the load increases beyond the allowable extent, the additional load is carried by the body of the rivets, which are subject to bending, crushing and shear.

Pain [7] has established that riveted joints also improve the damping capacity of structures. It is generally recognized that the damping capacity of jointed structures may be determined from the frictional loss energy caused by slip at the interfaces between the plates.

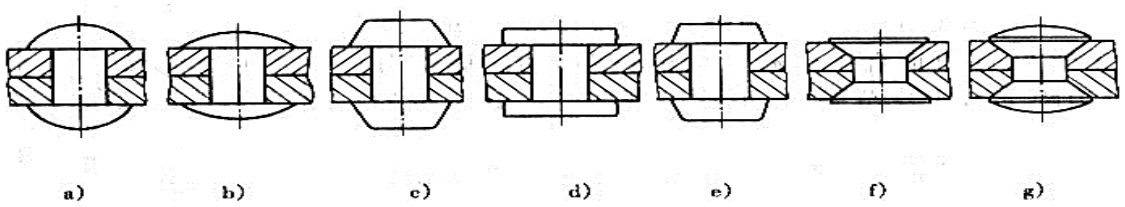

Figure 6: Different types of rivets after setting

The interfacial slip in joints is the major contributor to the inherent damping of most fabricated structures and hence, attention has to be focused on these influencing parameters in order to maximize the overall damping capacity of the riveted joints.

1.3 Joint properties

An important step towards the analysis and representation of the mode of vibration of machine is the analysis of spatial vibration behavior of the structure when vibrating in its resonance frequencies. In order to examine a machine from structural point of view it is necessary to provide a method by which a structural mode is abstracted from a machine. The modular construction system for machine tool has recently become important not only to rationalize their design and manufacturing procedure but also to evolve a feasible manufacturing system. Fundamental shape, main cross-sectional shape and function of structural modules and relation between adjacent structural configuration shows that a machine consists of many elementary

aggregate. This hierarchical property of machine structure suggests the possibility of defining a concrete model suitable for each joint in machine tool.

(1) The static stiffness of structures with joints is considerably lower than that of the equivalent solid structures and joint stiffness show the non-linear characteristics.

(2) The damping capacity of jointed structures is higher than that of equivalent solid one, but the natural frequency of jointed structures is less as compared to solid one.

(3) The characteristics mentioned above are in large dependence on the stiffness ratio of joint surrounding.

1.3.1 Static stiffness

The stiffness and the damping of the practical fabricated structures are not always linear because of the existence of a certain preload. The static stiffness of structures with joints is considerably lower than that of the equivalent solid structures and joint stiffness show the non-linear characteristics. Always, some of the stiffness of the structure is sacrificed due to the inclusion of joints, although this loss in stiffness is not allowed to be large if the joints are carefully designed. The use of joints has its own drawbacks causing fretting corrosion at the interfaces, reducing stiffness and presenting difficulty in analysis due to nonlinearity [8,9]. Beards [10] has pointed out that any loss of static stiffness of a structure will not necessarily affect the integrity of the structure if the joints are carefully designed.

1.3.2 Contact pressure

The contact pressure between the surfaces is generated by the clamping action of the joints and plays a vital role in the joint properties. Under such circumstances, the profile of the interface pressure distribution assumes a significant role, especially in the presence of slip for dissipation of vibration energy. This pressure is not uniform across the interface; rather it is maximum at the joint and decreases radially with the distance away from the joint. Due to this uneven pressure distribution, a local relative motion termed as micro-slip occurs at the interfaces of the connecting members. At the specified joint clamping pressure, sliding takes place on a micro scale and the Coulombs law of friction is assumed to be valid.

1.3.3 Friction Damping

The presence of friction in connecting joints has a strong impact on the system dynamics and largely contributes to the majority of the damping capacity of the system. It is understood that the joint friction arises only when the contacting layers tend to move relatively under the action of transverse vibration and serves as a catalyst for energy dissipation. For most analyses, the Coulomb's friction law is widely used to represent the dry friction at the contacting surfaces. Many authors have carried out an elaborate review of research on the effects of joint friction on structural damping in built-up structures [11-16].It takes place whenever two surfaces experience relative motion in the presence of friction. In case of a jointed structure, the relative motion between contacting layers is a function of normal load which arises from the tightening of the joints holding the components. When the joint is very loose, the normal load is insignificant and the contact surface experiences pure slip. Since no work is required to be done against friction, no energy is dissipated. On the other hand, when the joint is very tight, high normal loads cause

the whole contact interface to stick. This results in no energy dissipation again since no relative motion is allowed at the interfaces. For normal loads lying between these two extremities, energy is dissipated and the maximum value of energy dissipation occurs within this range. The damping caused by friction is non-linear and may be either positive or negative which means either stable sliding or self-excited oscillations (stick-slip). Measurement shows that damping depends upon slide way materials, velocity, lubricant and mass. The friction force generated between the joint interfaces is usually dependent on the materials in contact and proportional to the normal force across the interface.

1.3.4 Micro slip

Due to uneven pressure distribution, a local relative motion termed as micro-slip occurs at the interfaces of the connecting members. Mechanism of damping in a joint is not merely due to friction but is a complex one of micro and macro friction [17] and cyclic plastic deformation is likely to be predominant mechanism to which energy dissipation could be attributed.

(1) Macro-slip involving frictional damping

(2) Micro-slip involving very small displacement of asperities with respect to other surface.

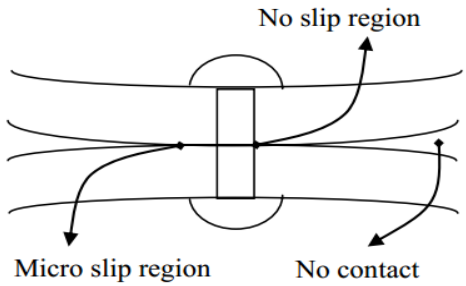

Figure 7: Mechanism of micro-slip at the jointed interface

Micro-slip is the normal mechanism by which mechanical joints dissipate energy and therefore, a better understanding of its phenomenon is required for the study of damping effects in the jointed structures. It generally occurs only at lower excitation levels. When the excitation level is increased, both micro- and macro-slips occur at the jointed interfaces. Usually, the macro-slip is avoided as it leads to structural damage of the joints. The contribution of the micro-slip on the overall system damping is significant in spite of its low magnitude and is generally promoted in structural joint designs.

1.4 Objective

Over the years, researchers have emphasized their studies on the development of mathematical models for the mechanism of damping and techniques to improve the damping capacity of laminated structures to control the adverse effects of vibrations. The energy dissipated in most real structures is often very small, so that an undamped analysis is sometimes realistic. When the damping is significant, its effect must be included in the analysis particularly when the dynamic study of a structure is required. The energy of the vibrating system is dissipated by various mechanisms and often more than one mechanism may be present at the same time. Although the knowledge on the friction joint is limited, efforts have been put in the present investigation to study the damping aspect of the friction joints in built-up structures.

In the present investigation, damping capacity of layered and jointed structures has been evaluated from analytical expressions developed in the investigation and compared experimentally for mild steel fixed beams with two or more layers under different conditions of excitation in order to establish the accuracy of the theory developed.

Chapter 2

2 Literature review

Conventional structural rivets are widely used in aircraft, transportation equipment, and other products requiring high joint strength. They are also used in the construction of buildings, boilers, bridges, and ships. The development of modern riveting machines has greatly expanded their use in fastening smaller components in a multitude of industrial products associated with the automotive, appliance, electronic, furniture, business machine, and other fields. Rivets have frequently replaced threaded fasteners in these applications because of lower installation cost. Significant initial tension is attainable in rivets by installing them at a red heat. The tension develops upon cooling and thermal contraction. Rivets are much cheaper than bolts, and modern high-speed riveting machines - some of which fasten over 1000 assemblies per hour - give low assembly cost. It is advantageous for any engineering structure to possess sufficient damping capacity so that any excessive vibration is suppressed to a reasonable limit thereby enhancing the life of the structures.

A feature common to all joints is that they dissipate energy when subjected to vibration. In practice, the joint effects can be very significant on the response of a fabricated structure. It is a general fact that the total damping in a structure is always much more than the sum of the material damping of individual elements of the structure. It is therefore recognized that the damping is largely caused due to the inclusion of mechanical joints or fasteners in the structure. As pointed out by Beards [18], up to 60% of the deformation and 90% of the damping in a fabricated structure arises from various joints. Most engineering structures are built up by connecting structural components through mechanical connections. Such assembled structures need sufficient damping to limit excessive vibrations under dynamic loads. The provision of

layers in association with joints encourages large damping in built-up structures. These connections are recognized as a good source of energy dissipation and greatly affect the dynamic behavior in terms of natural frequency and damping [11, 15, 19].The energy dissipation mechanism in a joint is a complicated phenomenon being largely influenced by the interface pressure and slip between the contacting surfaces. Although the energy dissipation is related to many physical phenomena, the friction between the layers is considered to be the most important factor [15]. It is always difficult for the theoretical assessment of damping arising in joints because of variations in the coefficient of friction under dynamic conditions.

Masuko et al. [20] and Nishiwaki et al. [21, 22] have found out the energy loss in jointed cantilever beams considering micro-slip and normal force at the interfaces. Olofsson and Hagman [23] have shown that the micro-slip at the contacting surfaces occur when an optimum frictional load is applied. They have also presented a model for micro-slip between the flat smooth and rough surfaces covered with ellipsoidal elastic bodies. Ying [24] has proposed a new generalized micro-slip model to study the effect of friction in joints for controlling the dynamic response of structures.

The friction in a joint arises from shearing between the parts and is governed by the tension in the bolt/rivet, surface properties and type of materials in contact [25]. Den Hartog [26] has analytically solved the steady state response of a simple friction-damped system with combined Coulomb and viscous friction.

The nature of pressure distribution across a beam layer is another important aspect affecting the damping capacity of jointed structures. Several workers have tried over the years to know the

actual pattern of pressure distribution at the interfaces due to the clamping action on the joint[20-22],[7,27,28,]. Many authors [29-34] have conducted experiments to know the exact distribution characteristics. These experiments have confirmed that the interface pressure is hardly constant in actual situation. In particular, Gould and Mikic [35] and Ziada and Abd [36] have reported that the pressure distribution at the interfaces of a bolted joint is parabolic in nature circumscribing the bolt which is approximately 3.5 times the bolt diameter. Recently, Nanda and Behera [37] have developed a theoretical expression for the pressure distribution at the interfaces of a bolted joint by curve fitting the earlier data reported by Ziada and Abd [36]. They have obtained an eighth order polynomial even function in terms of normalized radial distance from the centre of the bolt such that the function assumes its maximum value at the centre of the bolt and decreases radially away from the bolt. Using exact spacing of 2.00211 times the diameter of the connecting bolts, Nanda and Behera have been successful in simulating uniform interface pressure over the length of the beam. Thereafter, they have investigated the effect of interface pressure on the behavior of interfacial slip damping.

Damisa et al. have shown that under the action of dynamic loads, the factors like non-uniform pressure distribution as well as frequency variation have a significant effect on both the energy dissipation and logarithmic decrement associated with the mechanism of slip damping in layered structures [33]. The angle probe used by Minakuchi et al. [38] is more convenient to measure. They have found out the contact pressure between two layered beams of different thicknesses by establishing a relationship between the mean contact pressure and sound pressure of reflected waves. This method is widely accepted as the experimental results fairly agree with the theoretical ones. The present investigation uses the numerical data of Minakuchi et al. [38] to

obtain the theoretical expressions for non-uniform pressure at the interfaces of a jointed beam by curve fitting with MATLAB software.

The normal interfacial pressure across the clamped joint is not uniformly distributed. Under high pressure, the slip is small, while under low pressure the shear due to friction is small. An optimal clamping force exists somewhere between these two limits under which a joint dissipates maximum vibration energy. Beards [18] has looked into this aspect and recognized the existence of an optimum joint force for maximum energy dissipation.

Chapter 3

3 Theoretical analysis

Most structural problems are studied based on the assumption that the structure to be analyzed is either linear or nonlinear. In linear systems, the excitation and response are linearly related and their relationship is given by a linear plot as shown in Fig. For many cases, this assumption is more often valid over certain operating ranges. Working with linear models is easier from both an analytical and experimental point of view. For a linear system, the principle of superposition holds which means that doubling the excitation will double the levels of the response. For beams undergoing small displacements, linear beam theory is used to calculate the natural frequencies, mode shapes and the response for a given excitation. It is very clear from Fig. that the linear and nonlinear systems agree well at small values of excitation, while they deviate at higher levels. The nonlinear beam theory is used for larger displacements where the superposition principle is not valid [20]. The linear vibration theory is used when the beam is vibrated at small amplitudes and lower modes of vibration [2]. The present investigation mainly focuses on the study of damping of jointed fixed beams at lower excitation levels which can be considered as linear.

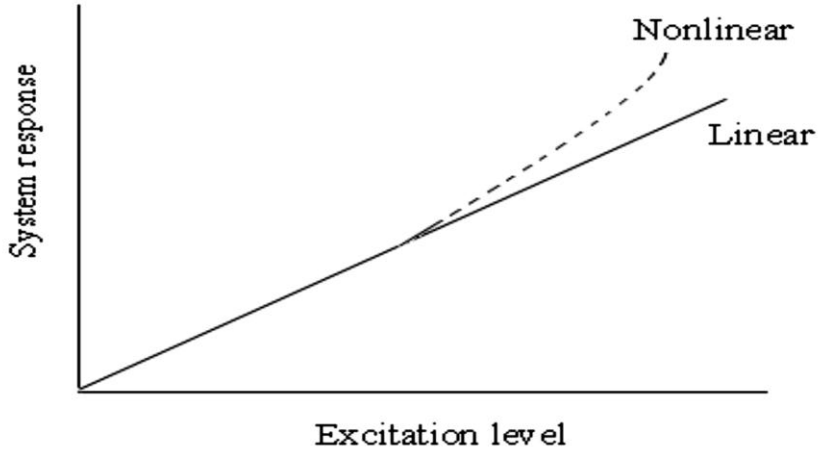

Figure 8: Comparison of Linear and nonlinear systems

3.1 Measurement of Structural Damping

There are several ways of expressing the damping in a structure. Out of which two ways are generally used by which damping measurements can be made:

1. Time-Response Method and
2. frequency-response methods

The basic difference between the two types of measurements is that the first type uses a time-response record of the system to estimate damping, whereas the second type uses a frequency-response record. Depending on the mathematical model of the physical problem, the above two methods are used to measure the damping capacity of the structures. Logarithmic decrement (δ) is determined using time domain method and the quality factor (Q) by frequency domain method. However, the other nomenclatures such as; damping ratio (ζ), specific damping capacity (ψ) and loss factor (η) are estimated from either of the above two methods for measuring the damping.

3.1.1 Logarithmic Decrement (δ)

The logarithmic decrement method is the most widely used time-response method to measure damping from the free-decay of the time history curve. When the structure is set into free vibration, the fundamental mode dominates the response since all the higher modes are damped out quickly. The logarithmic decrement represents the rate at which the amplitude of a free damped vibration decreases. The logarithmic damping decrement, a measure of the damping capacity of layered and jointed structures has been determined using the energy principle, considering the relative dynamic slip and the pressure distribution at the interfaces. These two vital parameters must be accurately assessed for correct evaluation of the damping capacity of such structures.

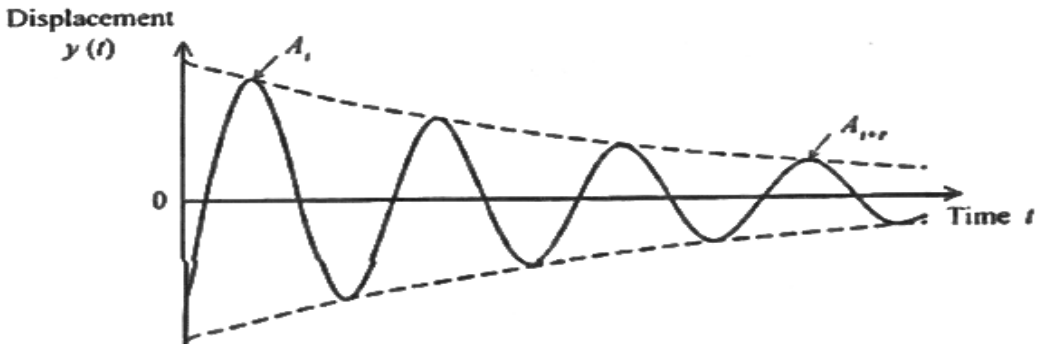

Figure 9: Time response graph showing the decay of amplitude

Thus, the logarithmic decrement δ is obtained as: $\delta=\ln\frac{x_1}{x_2} = \frac{2\pi\zeta}{\sqrt{1-\zeta^2}}$, where x_1 and x_2 are the successive amplitudes and ζ is the damping ratio.

For small damping, the above relation is approximated as; $\delta \simeq 2\pi\zeta$. Generally for low damping, it is preferable to measure the amplitudes of oscillations of many cycles so that an accurately measurable difference exists. In such a case, $\delta = \frac{1}{n}\ln\left(\frac{x_0}{x_n}\right)$, where x_0 , x_n and n are the amplitudes of first and last cycles and number of cycles, respectively.

3.1.2 Quality Factor (Q)

The half-power point bandwidth method is a frequency-domain method used to determine the damping in terms of quality factor (Q). This method is based on the magnitude curve of the frequency-response function. When a structure is subjected to a forced vibration by a harmonic exciting force, the ratio of maximum dynamic displacement (Xmax) at steady-state condition to the static displacement (Xs) under a similar force is called the Q factor. $Q = \frac{X_{max}}{X_s} = \frac{1}{2\zeta}$. The above equation shows that the Q factor is equal to the reciprocal of twice the damping ratio ζ.

Since a structure is excited into resonance at any of its modes, a Q factor can be determined for each mode. Systems with high Q factor have low damping and vice versa.

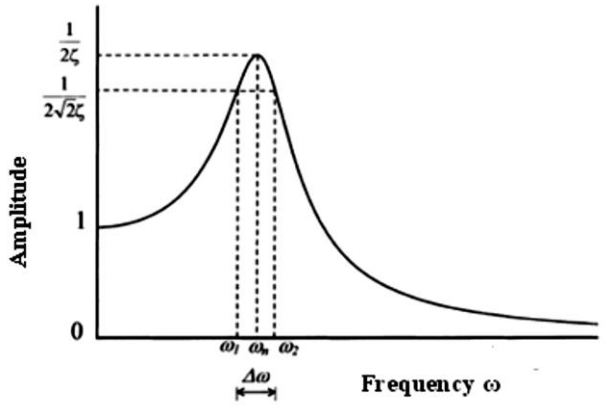

Figure 10: Q-factor method of damping measurement

If the static displacement (Xs) cannot be determined, the Q factor is found out using the half-power point method. The half-power points are those points on the response curve with amplitude 1.2 times the amplitude at resonance as presented in Fig. This method requires very accurate measurement of the vibration amplitude for excitation frequencies in the region of resonance. Once the maximum dynamic displacement (X_{max}) and resonant frequency (ω_n) have been located, the so-called half-power points are determined when the amplitude is $X_{max}/\sqrt{2}$ and the corresponding frequencies on either side of resonant frequencies, ω_1 and ω_2 are determined. Since the energy dissipated per cycle is proportional to the square of amplitude, the energy dissipated is reduced by 50% when the amplitude is reduced by a factor $1/\sqrt{2}$. Thus the Q factor is modified as: Q = $\frac{1}{2\zeta} = \frac{\omega_n}{\Delta\omega}$ where Δω is the frequency bandwidth at the half-power points.

3.1.3 Damping Ratio (ζ)

The damping ratio is another way of measuring damping which shows the decay of oscillations in a system after a disturbance. Many systems show oscillatory behavior when they are disturbed from their position of static equilibrium. Frictional losses damp the system and cause the oscillations to gradually decay to zero amplitude. The damping ratio provides a mathematical means of expressing the level of damping in a system. It is defined as the ratio of the damping constant to the critical damping constant.

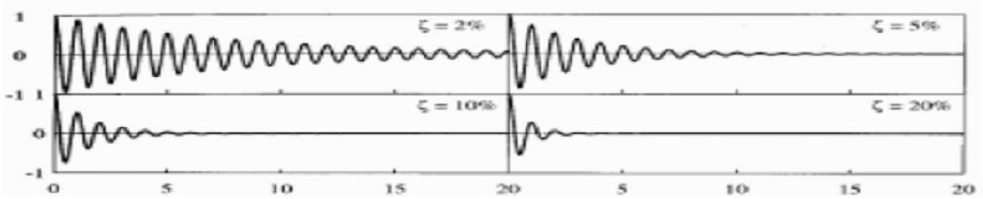

Figure 11: Free vibration of systems with different levels of damping

The rate at which the motion decays in free vibration is controlled by the damping ratio ζ, which is a dimensionless measure of damping expressed as a percentage of critical damping. Figure displays the free vibration response of several systems with varying levels of damping ratios. It is observed that the amplitude of vibration decays more rapidly as the value of the damping ratio increases.

3.1.4 Specific Damping Capacity (Ψ)

The damping capacity is defined as the energy dissipated per complete cycle of vibration. The energy dissipation per cycle is calculated from the damping force (f_d) and is expressed in the integral form as; $\Delta U = \oint f_d \, dx$**.** This is given by the area of the hysteresis loop in the displacement force-plane. The specific damping capacity (Ψ) is defined as the ratio of energy dissipated per cycle of vibration to the total energy of the system. If the initial (total) energy of the system is denoted by U_{max}, the specific damping capacity is given by: $\Psi = \frac{\Delta U}{U_{max}}$.

3.1.5 Loss Factor (η)

The loss factor η is the specific damping capacity per radian of the damping cycle and is widely used in case of visco-elastic damping. This is expressed as: $\eta = \frac{\Delta U}{2\pi U_{max}}$. It is noted that U_{max} is approximately equal to the maximum kinetic or potential energy of the system when the damping is low. Finally, the general relationship among various nomenclatures of damping measurement (valid for small values of damping) is given by: $\frac{1}{Q} = \frac{\psi}{2\pi} = 2\zeta = \frac{\delta}{\pi} = \eta = \frac{\Delta U}{2\pi U_{max}}$

3.2 Beam Theories

The beam is one of the fundamental elements of an engineering structure and finds application in structural members like helicopter rotor blades, spacecraft antennae, flexible satellites, airplane wings, gun barrels, robot arms, high-rise buildings, long span bridges, etc. These beam-like structures are typically subjected to dynamic loads. Therefore, studying the static and dynamic response, both theoretically and experimentally, of these structural components under various loading conditions would help in understanding and explaining the behavior of more complex and real structures. The popular beam theories in use today are:

1. Euler-Bernoulli beam theory and
2. Timoshenko beam theory.

Dynamic analysis of beams is generally based on one of the above beam theories. If the lateral dimensions of the beam are less than one-tenth of its length, then the effects of shear deformation and rotary inertia are neglected for the beams vibrating at low frequency. The no-transverse-shear assumption means that the rotation of cross section is due to bending alone. A beam based on such conditions is called Euler-Bernoulli beam or thin beam.

If the cross-sectional dimensions are not small compared to the length of the beam, the effects of shear deformation and rotary inertia are to be considered in the analysis. Timoshenko included

these effects and obtained results in accordance with the exact theory. The procedure presented by Timoshenko is known as thick beam theory or Timoshenko beam theory. The present investigation is based on the assumptions of Euler-Bernoulli beam theory as the beam is vibrated at low frequency and the dimensions of test specimens are much smaller in the lateral directions compared to length, thus satisfying the condition of thin beam theory.

3.3 Modeling of a Structure

It is essential to have a theoretical model to represent a structure in order to study its dynamic characteristics. Theoretical modeling of the present problem considers a continuous model approach using the Euler-Bernoulli beam theory.

A continuous model is characterized by a partial differential equation with respect to spatial and time coordinates which is often used for studying simple structures such as a uniform beam. Exact solutions of such equations are possible only for a limited number of problems with simple geometry, boundary conditions and material properties. However, real-life engineering structures are generally very complex in geometry, boundary conditions and material properties. For this reason, normally some kind of other approximate method is needed to solve a general problem.

The logarithmic damping decrement, a measure of damping capacity of layered and jointed structures, is usually determined by the energy principle taking into account the relative dynamic slip and the interfacial pressure between the contacting layers. These two vital influencing parameters are to be assessed accurately for correct evaluation of damping capacity, of such structures.

3.4 Dynamic Equations of Free Transverse Vibration of Fixed-Fixed Beams

Figure shows a fixed beam undergoing free vibration with transverse displacement y(x,t) . In formulating the dynamic equations, Euler-Bernoulli beam theory is used on the assumptions that the angular distortion due to shear is small in relation to bending deformation. This assumption is valid when the ratio of the length of beam to its depth is relatively large as in case of the present investigation.

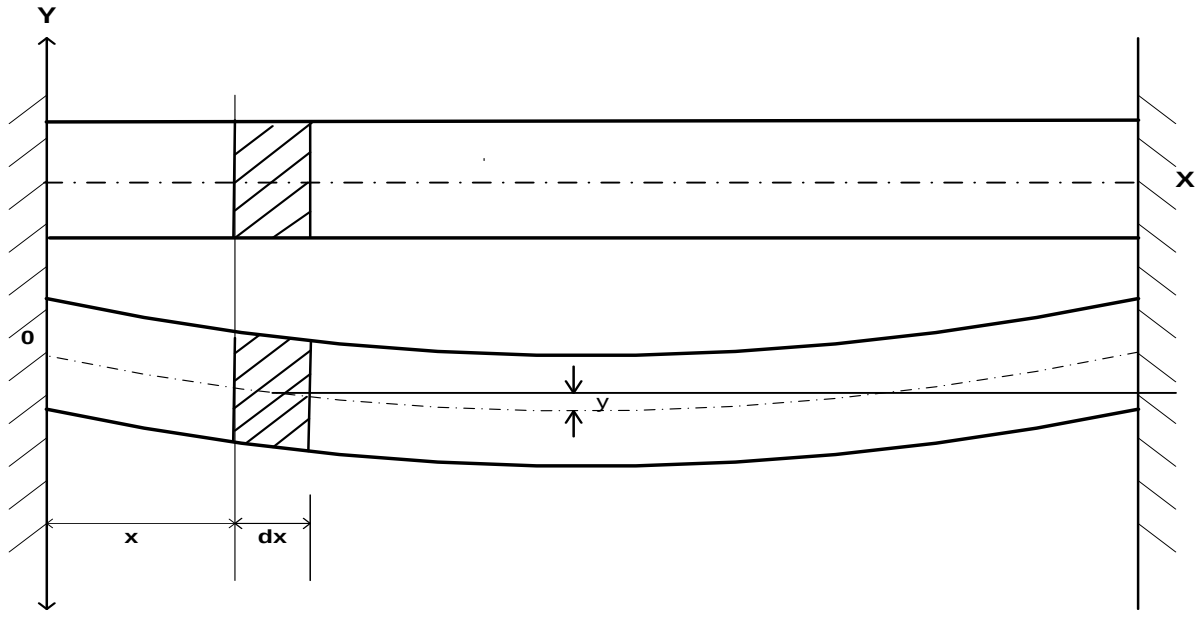

Figure 12: Differential analysis of the fixed-fixed beam

The beam vibration is governed by partial differential equations in terms of spatial variables x and time variable t. Thus, the governing differential equation for free vibration is given by:

$$EI\ \frac{d^4y}{dx^4} + \rho A\ \frac{d^2y}{dt^2} = 0 \qquad (1)$$

Where E, I, ρ and A are modulus of elasticity, second moment of area of the beam, mass density and cross-sectional area of the beam respectively. The free vibration given by eq.1 contains four

spatial derivatives and hence requires four boundary conditions for getting a solution. The presence of two time derivatives again requires two initial conditions, one for displacement and another for velocity.

Vibration in fixed-fixed beam is expressed as:

$$y(x, t) = G(x) * F(t) \quad (2)$$

where G(x) and F(t) are the space function and time function respectively.

Now the space function G(x) is given by :

$$G(x) = \frac{(\sin \lambda x - \sinh \lambda x)(\cos \lambda L - \cosh \lambda L) + (\cos \lambda x - \cosh \lambda x)(\sinh \lambda L - \sin \lambda L)}{(\cos \lambda L - \cosh \lambda L)} \quad (3)$$

Also, the time function F(t) is represented as:

$$F(t) = A \cos \omega_n t + B \sin \omega_n t \quad (4)$$

Where A and B are constants and and ω_n is the natural frequency. By putting the boundary conditions ,we get

$$A = \frac{y_0}{y(l/2)}, \text{ and } B=0$$

Substituting the eq.(3) and (4) in (2), we get:

$$y(x,t) = G(x) \frac{y_0}{y(l/2)} \cos \omega_n t \quad (5)$$

3.5 Evaluation of relative dynamic slip

It is assumed that each beam of the jointed fixed beam being vibrated, has the equal bending stiffness with the same bending condition. Moreover, each layer of the beam shows no extension of the neutral axis and no deformation of the cross-section. When the jointed fixed beam is given

an initial excitation at the mid span, the contacting surfaces undergo relative motion called micro-slip and at a particular position and time is given by Masuko et al. [15] as:

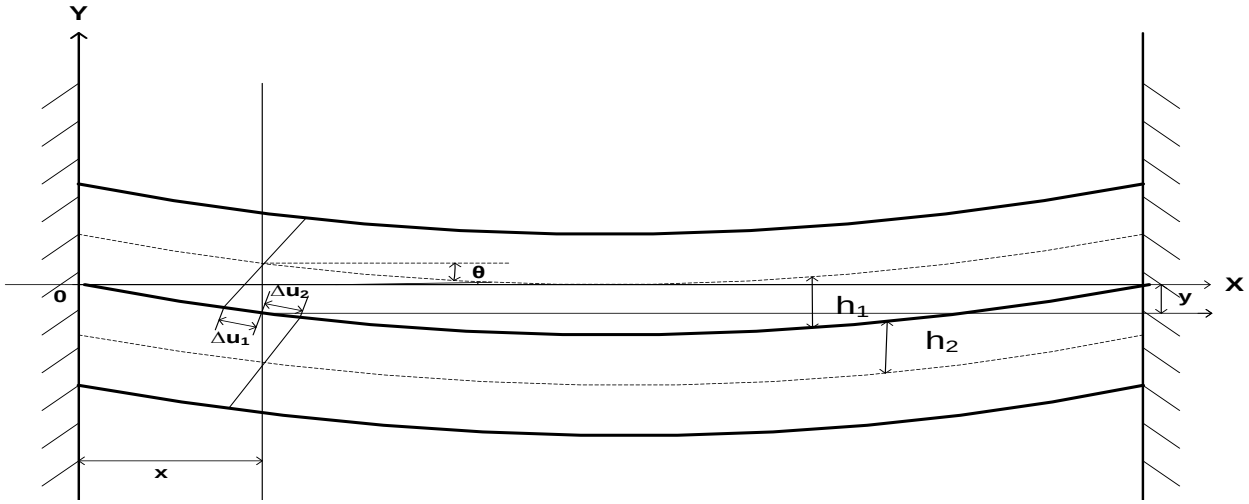

Figure 13: This relative displacement u(x, t) at any distance x from one end

The relative slip at the interface in the presence of friction during the vibration is given as:

$$u_r(x,t) = \propto u(x,t) = 2 \propto h\ tan\left[\frac{\partial y(x,t)}{\partial x}\right] \quad (6)$$

Where $\propto$ =slip ratio, here $(h1 = h2) = h$ = thickness of the beam, $y(x,t)$ = Deflection at a distance 'x' from one end, $u(x,t)$=dynamic slip without friction

3.6 Analysis Of Energy Dissipated Fixed-Fixed Beam

Energy is dissipated due to the relative dynamic slip at the interfaces. For the fixed-fixed beam with uniform pressure distribution at the interfaces, *p*, the energy loss due to the frictional force at the interfaces per half-cycle of vibration is given by:

$$E_{loss} = 2\int_0^{\frac{\pi}{\omega n}}\int_0^{\frac{L}{2}} \mu p b\left[\left\{\frac{\partial u_r(x,t)}{\partial t}\right\}\right] dxdt \quad (7)$$

Where μ = coefficient of kinematic friction, p = uniform pressure distribution at the interface, L=length of the beam, ω_n = natural frequency of vibration

The strain energy per half cycle of vibration is given by:

$$E_{ne} = \left(\frac{192EI}{L^3}\right) y^2 \left(\frac{L}{2}, 0\right) \tag{8}$$

where E, $\left[I = b\frac{(4h)^3}{12} \right]$ and y(l/2,0) are the modulus of elasticity, cross-sectional moment of inertia and transverse deflection at the midpoint of the fixed-fixed beam respectively.

where $\frac{E_{loss}}{Ene} = \left[\frac{8\mu bh\alpha y(\frac{l}{2},0)}{192(\frac{EI}{l^3}) y^2(\frac{l}{2},0)} \right]$ (9)

Replacing $192EI/l^3 = k_f$, i.e., the static bending stiffness of the layered and riveted fixed beam, the above equation (9) reduces to

$$\frac{E_{LOSS}}{E_{NET}} = \left[\frac{8\mu bhp\alpha}{k_f y(\frac{l}{2},0)} \right] \tag{10}$$

where k_f is the static bending stiffness of the fixed-fixed beam, y $\left(\frac{L}{2}, 0\right)$= transverse deflection at the mid-point of the fixed-fixed beam.

3.7 Evaluation Of Damping Ratio

The damping ratio, ψ, is expressed as the ratio of energy dissipated due to the relative dynamic slip at the interfaces and the total energy introduced into the system for rivets is found to be

$$\psi = \left[\frac{E_{loss}}{E_{losss} + E_{net}} \right] = \frac{1}{\left[1 + \frac{E_{net}}{E_{loss}} \right]} \tag{11}$$

where, E_{loss} and E_{ne} are the energy loss due to interface friction and the energy introduced during the unloading process Putting the values of $\frac{E_{loss}}{E_{ne}}$

$$\psi = \frac{1}{1 + \frac{\left[ky(\frac{l}{2},0) \right]}{[8\mu bph\alpha]}} \tag{12}$$

$$\psi = \frac{1}{1 + \frac{\left[ky(\frac{l}{2},0) \right]}{[2\mu bp\alpha h]}} \tag{13}$$

The above equations are used for calculating the damping ratio for the riveted joint structures.

3.8 Evaluation of Logarithmic decrement

Logarithmic decrement(δ), a measure of damping capacity, is defined as the natural logarithm of the ratio of two consecutive amplitudes in a given cycle.

$$\delta = \frac{1}{n} \ln \left(\frac{x_0}{x_n} \right) \tag{14}$$

Where x_0= amplitude of vibration of first cycle, x_n= amplitude of vibration of last cycle, n=number of cycles

Logarithmic decrement can also be written as;

$$\delta = \frac{1}{2}\left(\frac{E_{loss}}{E_{ne}}\right) \tag{15}$$

The logarithmic decrement for rivet joints is given as

$$\delta = \frac{1}{n}\ln\left(\frac{a_n}{a_{n+1}}\right) = \left[\ln\left\{\frac{1}{1-\psi}\right\}\right]/2 \tag{16}$$

By simplifying the above equation we get,

$$\delta = \frac{1}{2}\ln\left[1+\frac{8\mu\alpha pbh}{ky(\frac{l}{2},0)}\right] \tag{17}$$

3.9 Interface Pressure Distribution

A layered and jointed construction is made by means of rivets that hold the members together at the interfaces. Under such circumstances, the profile of the interface pressure distribution assumes a significant role, especially in the presence of slip, to dissipate the vibration energy. Consequently, it is necessary to examine the exact nature of the interface pressure profile and its magnitude across a beam layer for the correct assessment of the damping capacity in a jointed structure. This pressure distribution at the interfaces is due to the clamping of the rivets of the contacting members. When two or more members are pressed together by riveting, a circle of contact will be formed around the rivet with a separation taking place at a certain distance from the rivet hole . The contact between the connecting members develops an interface pressure. As established, the contact pressure at the jointed interface is non-uniform in nature being maximum at the rivet hole and decreases with the distance away from the rivet. This allows localized slipping at the interfaces while the overall joint remains locked. Minakuchi et al. [35] have found

that the interface pressure distribution due to this contact is parabolic with a circular influence zone circumscribing the rivet with diameter.

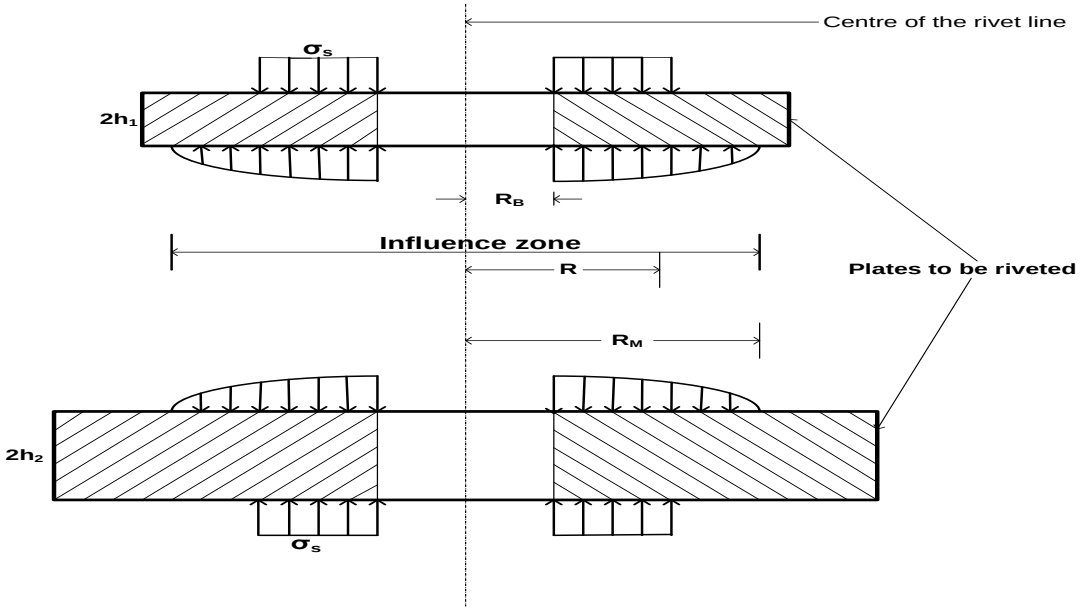

Figure 14: Free body diagram of a riveted joint showing the influence zone

3.9.1 Determination of Pressure Distribution at the Interfaces for Riveted

The interface pressure distribution under each rivet in a non-dimensional polynomial for layered and jointed structures is assumed as

$$P/\sigma_S = C_1(R/R_B)^{10} + C_2(R/R_B)^8 + C_3(R/R_B)^6 + C_4(R/R_B)^4 + C_5(R/R_B)^2 + C_6 \qquad (18)$$

Where P, σ_S, R and R_B are the interface pressure, surface stress on the layered and jointed structure due to riveting, any radius within the influencing zone and radius of the connecting rivet, respectively and constants C_1 to C_6 of the polynomial are evaluated from the numerical data of Minakuchi et al. [35] by curve fitting using MATLAB software as shown. The surface

stress σ_S depends upon the initial tension on the rivet (P) and the area under a rivet head (A′) and is evaluated from the relation

$$P/\sigma_S = P/A^{\cdot} \tag{19}$$

The distance between the rivets has been reduced in order to achieve the uniform pressure conditions.The above equation is an even function and a tenth order polynomial in terms of the normalized radial distance from the center of the rivet such that the function assumes its maximum value at the center of the rivet and decreases radially. It is evident that apart from the last two terms, values of the coefficients are relatively insignificant. This suggests for a linear profile for the pressure distribution across the interface. Damisa et al. [32] have used linear pressure profile in their analysis as an approximation. But a higher order polynomial for non-uniform interface pressure distribution has been used in the present investigation in order to obtain a good accuracy.

Table 1: Values of polynomial constants for different thickness ratios

THICKNESS OF PLATES	1	1.5	2
CONSTANT VALUES	c_6=0.14581228e-5 c_5=-0.57951686e-4 c_4=0.60446153e-3 c_3=0.30852824e-2 c_2=-0.95814172e-1 c_1=0.53777732	c_6=-1.737236e-7 c_5=1.398793e-5 c_4=-0.458813e-3 c_3=0.817021e-2 c_2=-0.877333e-1 c_1=0.488330	c_6=-0.7419798e-7 c_5=0.74507972e-5 c_4=-0.29801024e-3 c_3=0.62164809e-2 c_2=-0.74592085e-1 c_1=0.46039144
UNIFORM DISTANCE(R/R_B)	2.3539	2.4030	2.4340
AVERAGE PERSSURE	0.39032425	0.4055	0.4069

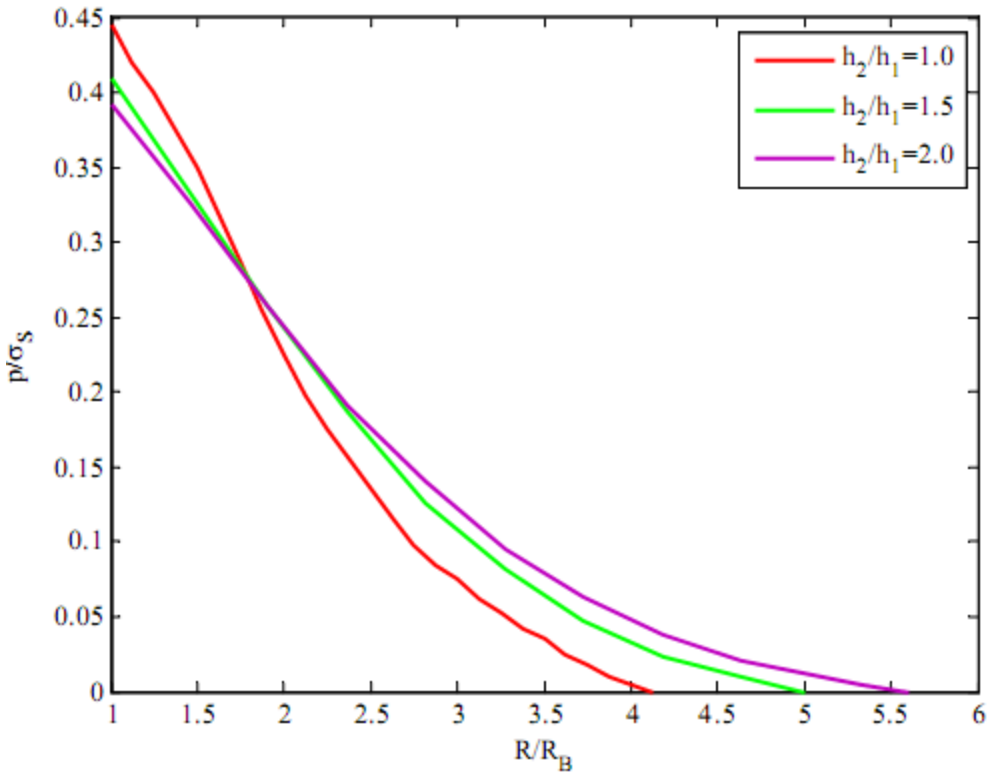

Figure 15: Variation of Pressure distribution (P/σ s) of different thickness of different distance (R/RB).—Theoretical.

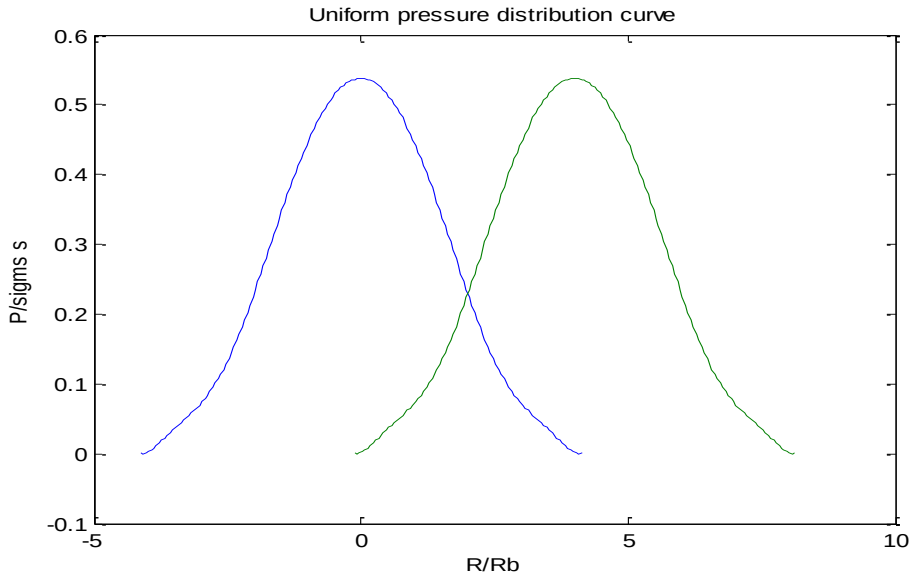

Figure 16: Uniform pressure distribution of riveted joints

Chapter 4

4 Experimental analysis

The experimental study of damping becomes necessary as the theoretically computed results of a machine or structure may be different from that of the actual values due to the various assumptions made in the analysis. Unlike mass and stiffness properties, damping is purely a dynamic characteristic of a system which needs to be measured by conducting the dynamic tests on a structure. In order to evaluate the effect of different parameters on damping capacity of various types of riveted joint beams, experiments were carried out with a simple experimental set-up.

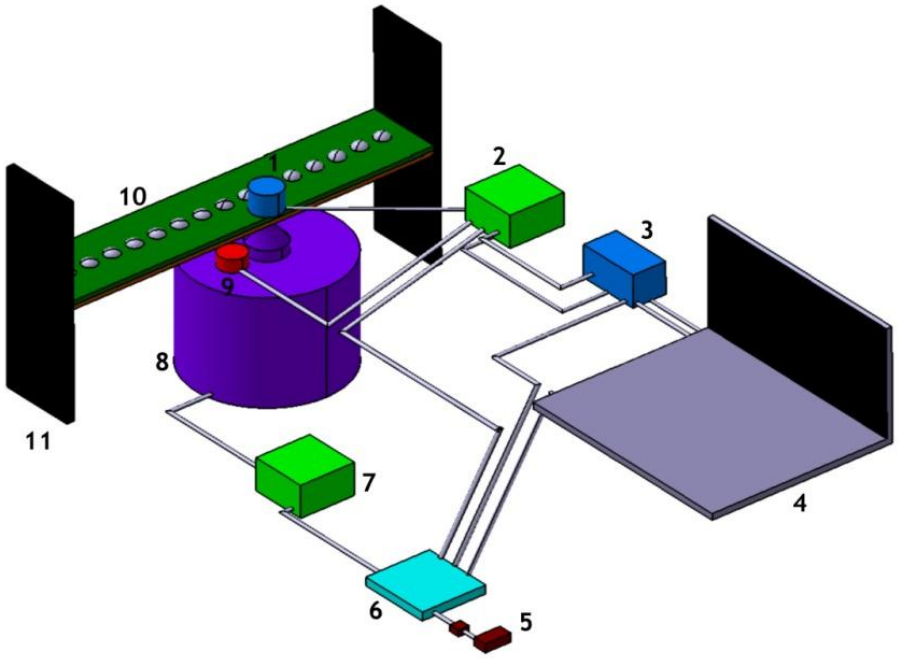

Figure 17: Schematic diagram of the experimental set-up

1.Output vibration pickup 2.Amplifier 3.Vibration acquisition 4.Vibration analyzer

5.Power supply 6.Distribution box 7.Power amplifier 8.Vibration generator

9.Input excitation pickup 10.Riveted beam 11.Fixed end

4.1 Set-up of the experiment:

The set-up consists of a frame work fabricated from steel channel sections by welding. The frame is grouted to a heavy and rigid concrete base by means of foundation bolts and it has the provision of slotted guide ways to accommodate the beams of different lengths. The frame has the provision to hold the fixed end of the cantilever beam specimens tightly and rigidly in order to ensure perfect cantilever condition. To attain the perfect fixed condition, we need to use the C-clamp and the packing materials to fix the other end of the beam rigidly. This clamping is achieved using a mechanical vice. The vice working on the screw-jack principle consists of a base plate and a spindle with internal and external threading. An arm is attached to this spindle at the upper end. On rotating the arm, it moves axially downward and imparts the necessary clamping force to the base plate thereby holding the specimen to achieve a perfect cantilever condition. The base plate prevents the rotation of the specimens while applying the fixed end load. A spring loaded exciter is used to initiate vibration at the free end of the specimens with predetermined amplitudes. The use of spring in the exciter ensures zero initial velocity of the specimen at the time of excitation. It is provided with dial gauge which is calibrated to read the initial amplitudes of excitation, mounted to a vertical stand with magnetic base.

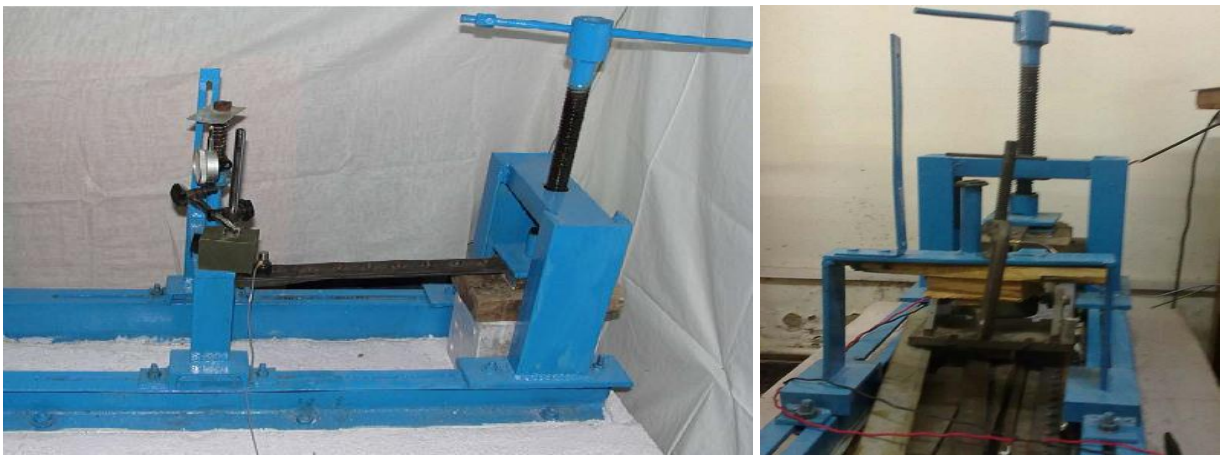

Figure 18: side view and front view of the experimental set-up

4.2 Preparation of Specimens:-

The test specimens of different sizes are prepared from the same stock of commercial mild steel flats as presented in Tables 2. Equi-spaced rivets of 10mm diameter are used to fabricate two layered specimens with a constant clamping force. Moreover, multi-layered specimens made up of mild steel are fabricated from 10 mm diameter connecting rivets. For all these specimens, the distance between the consecutive rivets is so arranged that their influence zone just touches each other at the point of separation. The width and length of the specimens are also taken from the rivet diameter and beam thickness ratio as per the zone of influence. The length of the specimens has also been varied accordingly in order to accommodate different number of rivets.

Figure 19: The photographs of a few specimens used in the experiments

Table 2: Details of mild steel specimens used in the experiment for the thickness ratio 1.0

Width * Thickness (mm*mm)	Number of layers	Type of specimen	Diameter of rivet(mm)	Number of rivets	Fixed beam span(mm)
24.8*(4+4)	2	jointed	8	6	148.8
24.8*(4+4)	2	Jointed	8	8	198.4
24.8*(4+4)	2	Jointed	8	10	248.0
24.8*(5+5)	2	Jointed	8	12	297.6

Table 3: Details of mild steel specimens used in the experiment for the thickness ratio 1.5

Width * Thickness (mm*mm)	Number of layers	Type of specimen	Diameter of rivet(mm)	Number of rivets	Fixed beam span(mm)
25*(4.5+3)	2	Jointed	10	6	150
25*(3+2)	2	Jointed	10	8	200
25*(4.5+3)	2	Jointed	10	10	250
25*(4.5+3)	2	Jointed	10	14	300

Table 4: Details of mild steel specimens used in the experiment for the thickness ratio 2.0

Width * Thickness (mm*mm)	Number of layers	Type of specimen	Diameter of rivet(mm)	Number of rivets	Fixed beam span(mm)
25*(4+2)	2	Jointed	12	8	194.4
25*(6+3)	2	Jointed	12	10	243
25*(6+3)	2	Jointed	12	12	291.6

Before clamping the specimens with rivets, the interfaces of the contacting members are cleaned properly to obtain perfect contact at the mating surfaces. The usual rivet consists of a solid cylindrical shank with a head at one end.

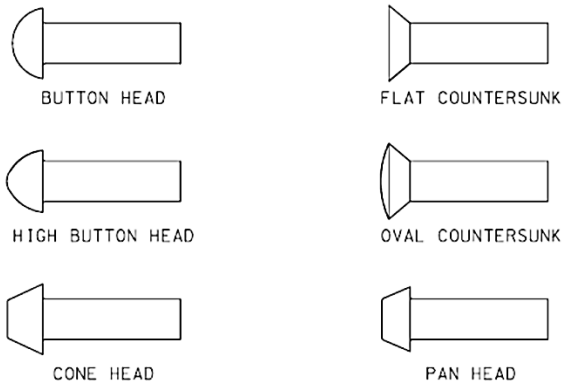

Figure 20: different types of rivet heads

The button head with power riveting technique has been used in the present investigation to clamp the beams. The hot rivet is inserted into the hole and a head is formed on the blunt end with a pneumatic pressure with the help of a die. The shank of the rivet is compressed causing it to expand and fill the hole almost completely. The rivet shrinks on cooling, thereby creates a clamping force between the connecting parts.

The specimen will be safe under the specified operating conditions which are mentioned below:

(1) Safe operating temperature: - + 10C to + 50C

(2) Temperature range for which specimen hold good: - + 20C to + 30C

4.3 Equipment used

To measure the logarithmic damping decrement, natural frequency of vibration of different specimen the following instruments were used as shown in circuit diagram fig:-

(1) Power supply unit

(2) Vibration pick-up

(3) Load cell

(4) Oscilloscope

(5) Dial gauge

4.3.1 Oscilloscope:

A digital storage oscilloscope as shown in Figure 21, is widely used for the processing and display of vibration signals and has a display screen, numerous input connectors, control knobs and buttons on the front panel. The signal to be measured is fed to one of the connectors. It plots a two dimensional graph of the time history curve.

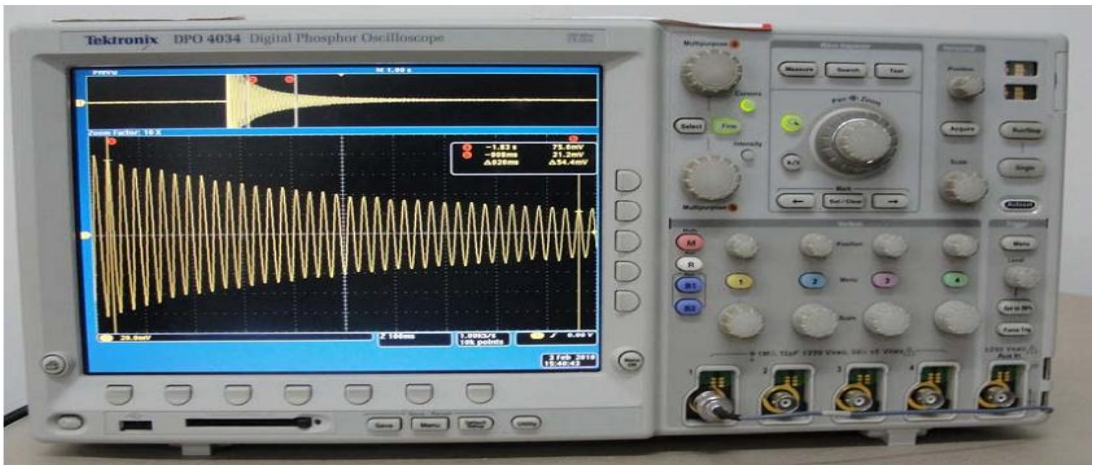

Figure 21: Digital storage oscilloscope

An oscilloscope measures two things:

1. Amplitude in time domain
2. Amplitude in frequency domain

4.3.1.1 Specifications of the oscilloscope used are as follows:

DPO 4000 series Oscilloscope

Input Voltage: 100 V to 240 V±10%

Input Power Frequency: 47 Hz to 66 Hz (100 V to 240 V)

400 Hz (100 V to 132 V)

Power Consumption: 250 W maximum

Weight: 5 kg (11 lbs), standalone instrument

Clearance: 51 mm (2 in)

Operating Temperature: 0 to 50 C

High Operating Humidity: 40 to 50 C, 10 to 60% RH

Low Operating Humidity: 0 to 40C, 10 to 90% RH

Operating Altitude: 3000 m (about 10,000 ft)

Operating Random Vibration: 0.31 GRMS, 5 – 500 Hz, 10 minutes per axis, 3 axes (30 minutes total)

Pollution Degree: 2, Indoor use only

4.3.1.2 Working principle:

An electron beam is swept across a phosphorescent screen horizontally (X direction) at a known rate (perhaps one sweep per millisecond). An input signal is used to change the position of the beam in the Y direction. The trace left behind can be used to measure the voltage of the input signal (off the Y axis) and the duration or frequency can be read off the X axis. An oscilloscope is a test instrument which allows you to look at the 'shape' of electrical signals by displaying a graph of voltage against time on its screen. A graticule with a 1cm grid enables you to take measurements of voltage and time from the screen. The graph is the trace and is drawn by a beam of electrons striking the phosphor coating of the screen making it emit light, usually green or blue. This is similar to the way a television picture is produced. Oscilloscopes contain a vacuum tube with a cathode (negative electrode) at one end to emit electrons and an anode (positive electrode) to accelerate them so they move rapidly down the tube to the screen. This arrangement is called an electron gun. The tube also contains electrodes to deflect the electron beam up/down and left/right. The electrons are called cathode rays because they are emitted by the cathode and this gives the oscilloscope its full name of cathode ray oscilloscope or CRO.

A dual trace oscilloscope can display two traces on the screen, allowing you to easily compare the input and output of an amplifier for example. It is well worth paying the modest extra cost to have this facility.

4.3.1.3 Connecting an oscilloscope:

The Y INPUT lead to an oscilloscope should be a co-axial lead and the diagram shows its construction. The central wire carries the signal and the screen is connected to earth (0V) to shield the signal from electrical interference (usually called noise). Oscilloscopes have a BNC socket for the y input and the lead is connected with a push and twist action, to disconnect you need to twist and pull. An oscilloscope is connected like a voltmeter but you must be aware that the screen (black) connection of the input lead is connected to mains earth at the oscilloscope! This means it must be connected to earth or 0V on the circuit being tested.

4.3.1.4 Obtaining a clear and stable trace

Once you have connected the oscilloscope to the circuit you wish to test you will need to adjust the controls to obtain a clear and stable trace on the screen:

- The Y AMPLIFIER (VOLTS/CM) control determines the height of the trace. Choose a setting so the trace occupies at least half the screen height, but does not disappear off the screen.
- The TIMEBASE (TIME/CM) control determines the rate at which the dot sweeps across the screen. Choose a setting so the trace shows at least one cycle of the signal across the screen. Note that a steady DC input signal gives a horizontal line trace for which the time base setting is not critical.
- The TRIGGER control is usually best left set to AUTO.

4.3.1.5 Measuring voltage and time period:

The shape of this graph is determined by the nature of the input signal.

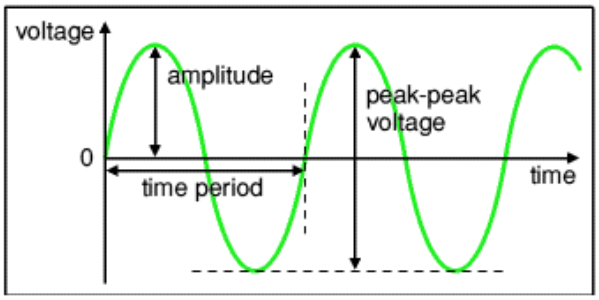

Figure 22: The trace on an oscilloscope screen is a graph of voltage against time.

In addition to the properties labeled on the graph, there is frequency which is the number of cycles per second. The diagram shows a sine wave but these properties apply to any signal with a constant shape.

- Amplitude is the maximum voltage reached by the signal. It is measured in volts, V.
- Peak voltage is another name for amplitude.
- Peak-peak voltage is twice the peak voltage (amplitude). When reading an oscilloscope trace it is usual to measure peak-peak voltage.
- Time period is the time taken for the signal to complete one cycle. It is measured in seconds (s), but time periods tend to be short so milliseconds (ms) and microseconds (μs) are often used. 1ms = 0.001s and 1μs = 0.000001s.
- Frequency is the number of cycles per second. It is measured in hertz (Hz), but frequencies tend to be high so kilohertz (kHz) and megahertz (MHz) are often used.

  1kHz = 1000Hz and 1MHz = 1000000Hz.

4.3.1.6 Voltage:

Voltage is shown on the vertical y-axis and the scale is determined by the Y AMPLIFIER (VOLTS/CM) control. Usually peak-peak voltage is measured because it can be read correctly even if the position of 0V is not known. The amplitude is half the peak-peak voltage. To read the amplitude voltage directly you must check the position of 0V (normally halfway up the screen): move the AC/GND/DC switch to GND (0V) and use Y-SHIFT (up/down) to adjust the position of the trace if necessary, switch back to DC afterwards so you can see the signal again. Voltage = distance in cm × volts/cm.

4.3.1.7 Time period:

Time is shown on the horizontal x-axis and the scale is determined by the TIMEBASE (TIME/CM) control. The time period (often just called period) is the time for one cycle of the signal. The frequency is the number of cycles per second, frequency = 1/time period Ensure that the variable time base control is set to 1 or CAL (calibrated) before attempting to take a time reading.

4.3.2 Velocity Transducer:

The velocity pickup is a very popular transducer or sensor for monitoring the vibration of rotating machinery. This type of vibration transducer installs easily on machines, and generally costs less than other sensors. For these two reasons, this type of transducer is ideal for general purpose machine applications. Velocity pickups have been used as vibration transducers on rotating machines for a very long time, and they are still utilized for a variety of applications today. Velocity pickups are available in many different physical configurations and output sensitivities.

4.3.2.1 Theory of Operation

When a coil of wire is moved through a magnetic field, a voltage is induced across the end wires of the coil. The induced voltage is caused by the transferring of energy from the flux field of the magnet to the wire coil. As the coil is forced through the magnetic field by vibratory motion, a voltage signal representing the vibration is produced.

4.3.2.2 Signal Conventions

A velocity signal produced by vibratory motion is normally sinusoidal in nature. In other words, in one cycle of vibration, the signal reaches a maximum value twice in one cycle. The second maximum value is equal in magnitude to the first maximum value, but opposite in direction. By definition velocity can be measured in only one direction. Therefore, velocity measurements are typically expressed in zero to peak, RMS units. RMS units may be specified on permanent monitor installations to allow correlation with information gathered from portable data collectors. Another convention to consider is that motion towards the bottom of a velocity transducer will generate a positive going output signal. In other words, if the transducer is held in its sensitive axis and the base is tapped, the output signal will go positive when it is initially tapped.

4.3.2.3 Construction:

The velocity pickup is a self-generating sensor requiring no external devices to produce a vibration signal. This type of sensor is made of three components: a permanent magnet, a coil of wire, and spring supports for the coil of wire. The pickup is filled with an oil to dampen the spring action. Due to gravity forces, velocity transducers are manufactured differently for horizontal or vertical axis mounting. With this in mind, the velocity sensor will have a sensitive axis that must be considered when applying these sensors to rotating machinery. Velocity sensors are also susceptible to cross axis vibration, which if great enough may damage a velocity sensor.

Wire is wound onto a hollow bobbin to form the wire coil. Sometimes, the wire coil is counter wound (wound one direction and then in the opposite direction) to counteract external electrical fields. The bobbin is supported by thin, flat springs to position it accurately in the permanent magnet's field.

4.3.3 Dial indicator:

Dial indicator are instruments used to accurately measure a small distance. They may also be known as a dial gauge, Dial test indicator (DTI), or as a "clock". They are named so because the measurement results are displayed in a magnified way by means of a dial. Dial indicator may be used to check the variation in tolerance during the inspection process of a machined part, measure the deflection of a beam or ring under laboratory conditions, as well as many other situations where a small measurement needs to be registered or indicated.

Figure 23: Dial gauge with magnetic base stand

A high precision dial gauge mounted on a stand with magnetic base is used to record the amplitude of vibration given at the tip of the specimen. The dial gauge as shown in Fig. is shock proof and can measure the amplitude of excitation in the range of 0.01 to 10 mm.

4.3.4 Accelerometer

The accelerometer is a device that transforms changes in mechanical quantities (such as displacement, velocity or acceleration) into changes in electrical quantities (such as voltage or current). One end of the accelerometer is held magnetically to the vibrating surface and the other end is connected to one of the connectors of the storage oscilloscope.

Figure 24: Vibration pick-up (accelerometer)

Specifications:

Type: MV-2000

Make: NAL, Bangalore, India

Optional gap: 2 mm

Coil resistance: 1000 ohms

Operating temperature: 10 to 40 degree centigrade

Dynamic frequency range: 2 c/s to 1000c/s

Vibration amplitude: ±1.5 mm maximum

Weight: 130 grams

4.4 Testing Procedure

The tests were performed in the prevailing laboratory environment. In order to perform the experiments, the specimens are rigidly mounted to the support as discussed earlier. At first, the Young's modulus of elasticity and static bending stiffness are measured by carrying out static deflection tests. These measured values are subsequently used for the theoretical evaluation of logarithmic decrement of all the specimens. Later, the experimental logarithmic decrement is calculated from the time history curve of decaying signals.

4.4.1 Measurement of Young's Modulus of Elasticity (E)

As mentioned in the preceding paragraph, the Young's modulus of elasticity (E) of the specimen material is found out by conducting static deflection tests. For this purpose, few samples of solid beams are selected from the same stock of mild steel flats. These specimens are mounted on the same experimental set-up rigidly so as to ensure perfect fixed boundary conditions as mentioned earlier. Static loads (W) are applied at the mid span of the beam arrangement and the corresponding deflections (Δ) are recorded. The Young's modulus for the specimen material is then determined using the expression $E = \left(\frac{WL^3}{192\Delta I}\right)$. Young's modulus of specimen materials (Mild steel) is 196.0 E(GPa)

4.4.2 Measurement of Static Bending Stiffness (k)

It is a well-known fact that the stiffness of a jointed beam is always less compared to an equivalent solid one. It means that the incorporation of joints to assemble layers of beams is accompanied by a decrease in the stiffness. The amount of reduction in the stiffness is quantified

by a factor called stiffness ratio which is defined as the ratio of the stiffness of a jointed beam (k) to that of an identical solid one (k′). The stiffness ratio is inversely related to the number of layers used in the jointed specimen. Its exact assessment carries much significance in the theoretical evaluation of logarithmic decrement. The same static deflection tests as used in case of Young's modulus are performed to measure the actual stiffness (k) of a jointed specimen using the relation $= w/\Delta$.

4.4.3 Measurement of Damping (δ)

After finding out the Young's modulus and static bending stiffness of the specimen materials, the tests are further conducted on the same set of specimens for evaluating the logarithmic decrement. The test specimens are first rigidly mounted on the set-up one after another. The test procedure is essentially the same for all the cases. A spring loaded exciter is used to excite the specimens at the free ends. The excitation is imparted for a range of beam-tip amplitudes varying from 0.1 to 0.5 mm in steps of 0.1 mm. For a particular test specimen, the beam is deflected and released to oscillate at its first mode of free vibration. The beam response is sensed by a contacting-type accelerometer attached to the tip of the beam. One end of the accelerometer is held magnetically to the vibrating surface of the specimen and the other is connected to one of the connectors of the storage oscilloscope. The output from the accelerometer is proportional to the frequency and amplitude of vibration. This output signal is fed to a digital storage oscilloscope for processing and display. The data is then analyzed to determine the natural frequency and damping characteristics of the beam structure.

Figure shows the block diagram of the basic vibration measurement scheme used in the present study. The decaying signal is recorded on the screen of the storage oscilloscope indicating that the energy dissipation is taking place. The cause of energy dissipation may be due to different effects such as material, joint friction and support damping. However, it is assumed that all the energy dissipation is due to the joint friction only.

Figure 25: Basic scheme of vibration measurement

Several techniques are used to quantify the level of damping in a structure as discussed in the literature review. Out of them, the logarithmic decrement technique is the most popular time-response method used for measuring the damping. The logarithmic decrement represents the rate at which the amplitude of a free damped vibration decreases. As the structure is considered to vibrate with small excitation level in the low and moderate frequency range, this method produces fairly good results for lightly damped linear systems. In this method, the structure is set into free vibration with the fundamental mode dominating the response since all the higher modes are damped out quite quickly. The vibration response of the specimen is picked up by the accelerometer and a time history curve showing the decay of amplitude is displayed on the digital storage oscilloscope

Design of experimental set-up for measurement of damping requires some primary consideration. It is assumed that the energy losses due to support friction, air drag, connecting wires, accelerometer mountings etc., are neglected.

Secondly, proper care has been taken while preparing the specimens, assembling the test rig and conducting the experiments. The connecting members of any test specimen should be flat with perfect contact at the interfaces. This will ensure identical pressure distribution under each connecting rivet along the interfaces so that proper energy dissipation takes place. While mounting the specimen in the test rig, sufficient clamping has to be provided in order to achieve a perfect cantilever condition which will greatly reduce the errors due to support damping. Further, some errors may build up while giving the initial excitation which may not be instantaneous. This may not ensure perfect sinusoidal waveforms thus containing some harmonic contents. All these factors should be considered during experimentation in order to minimize the errors.

Chapter 5

5 Results and Discussions

5.1 Graphs:

The following figures and graphs have been obtained after performing numerous experiments on the mild steel specimens of varying dimensions as described earlier. And the following chapter gives the conclusions that have been made after analyzing all the data and from the points of the discussion.

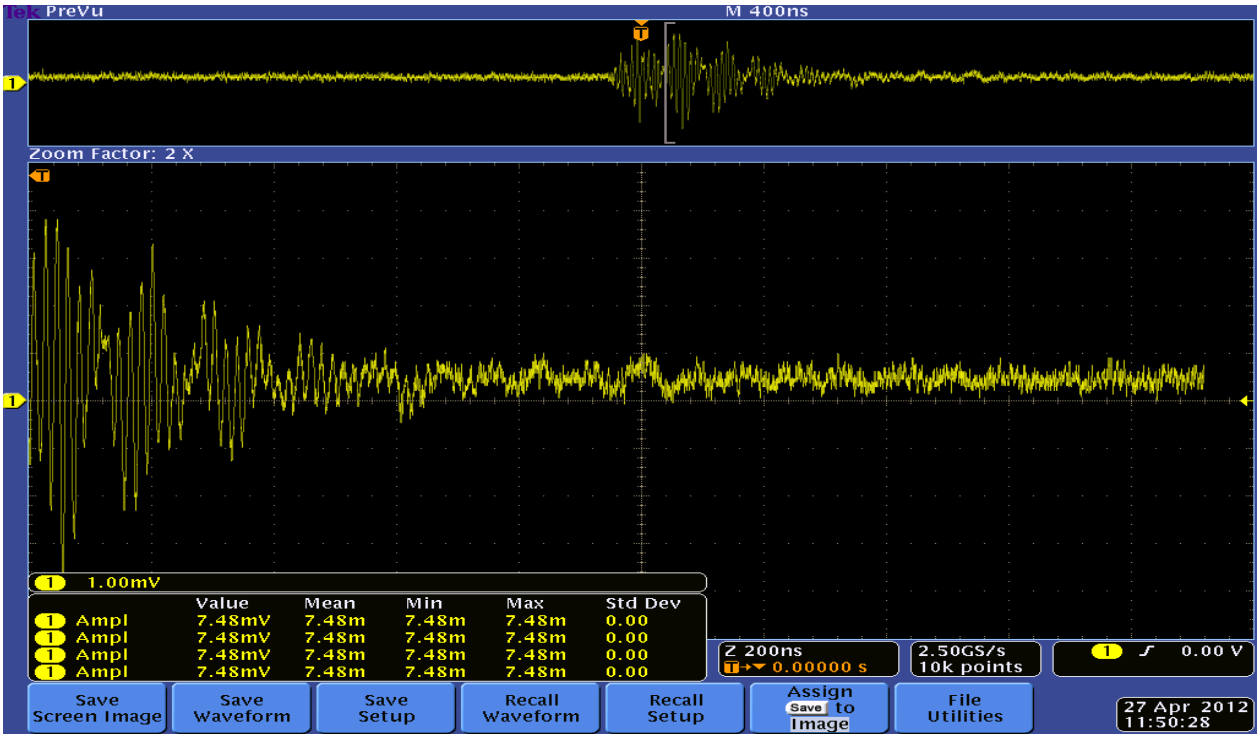

Figure 26: Screen-shot of oscilloscope while performing an experiment on fixed beam set-up

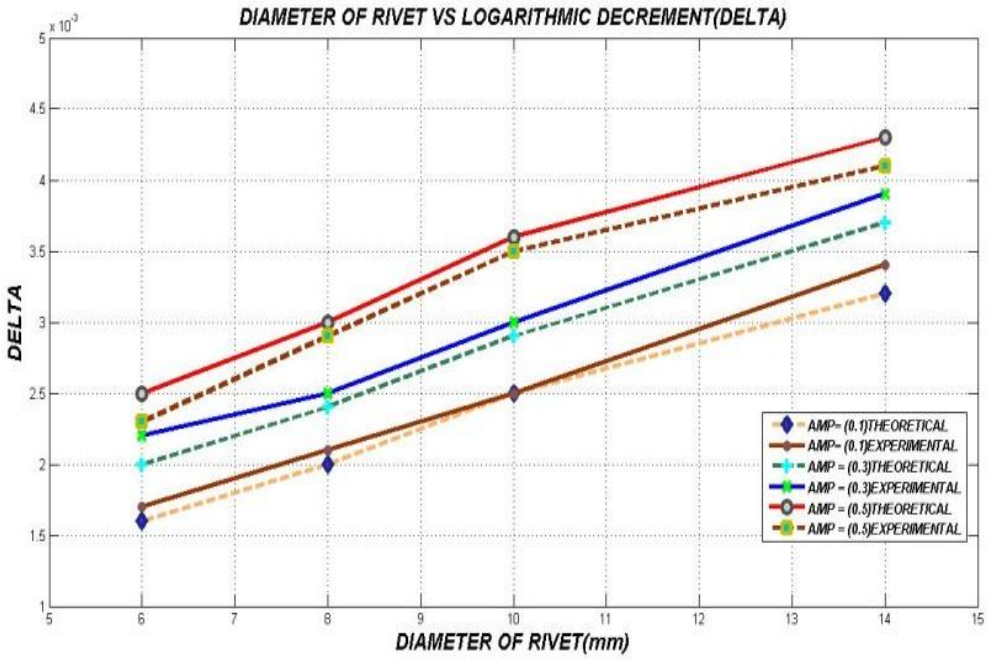

Figure 27: Variation of logarithmic decrement with the diameter of rivet at different amplitudes of excitation (y) for mild steel specimen of fixed-fixed beam having a thickness ratio of 1.0.

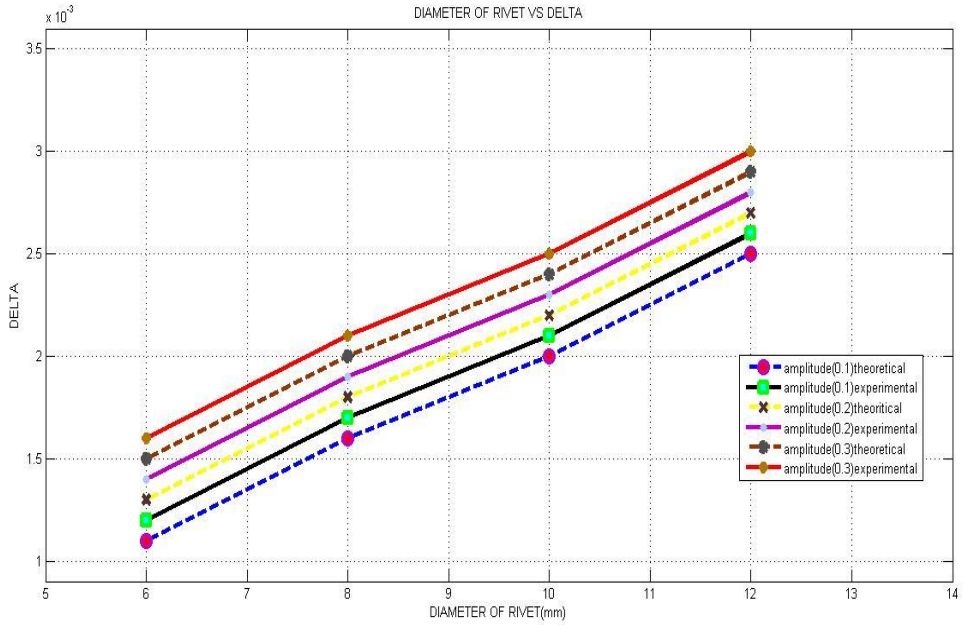

Figure 28: Variation of logarithmic decrement with the diameter of rivet at different amplitudes of excitation (y) for mild steel specimen of fixed-fixed beam having a thickness ratio of 1.5.

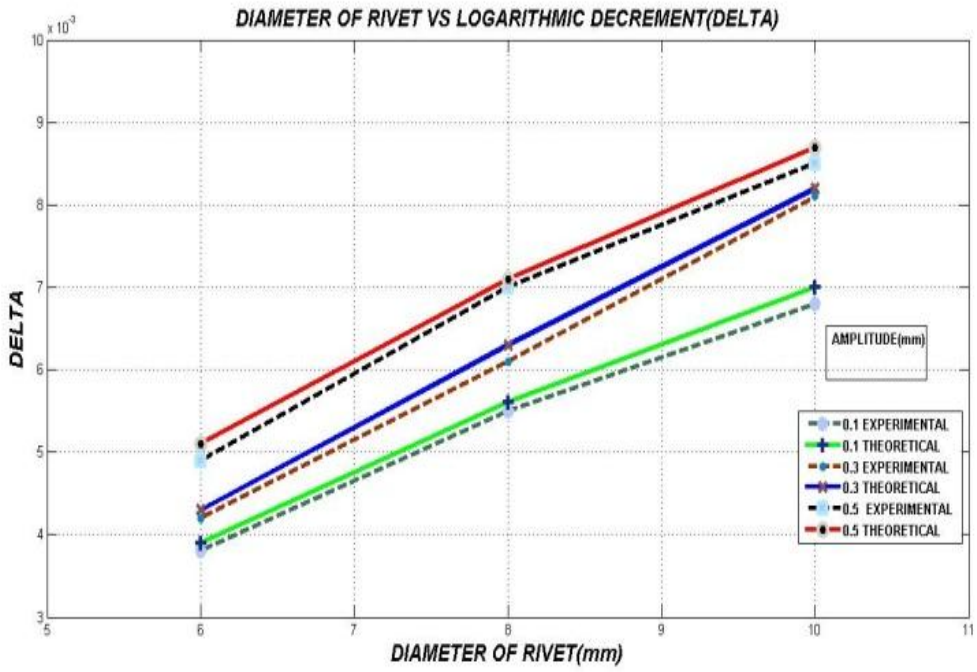

Figure 29: Variation of logarithmic decrement with the diameter of rivet at different amplitudes of excitation (y) for mild steel specimen of fixed-fixed beam having a thickness ratio of 2.0.

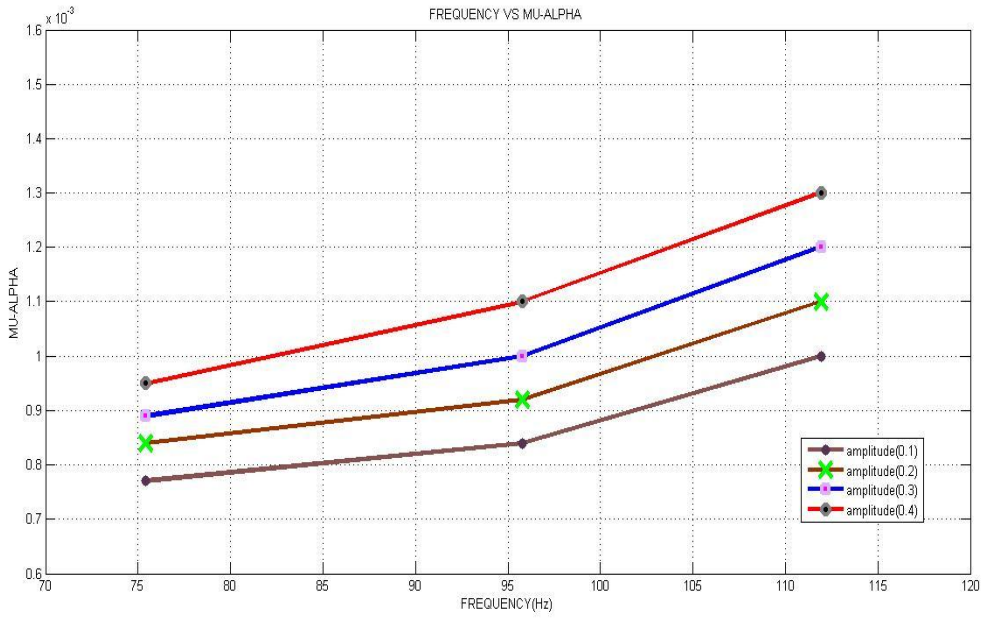

Figure 30: Variation of α.μ with the frequency of a beam having thickness ratio 1.0 for fixed-fixed beam at different initial amplitudes of excitation (y)

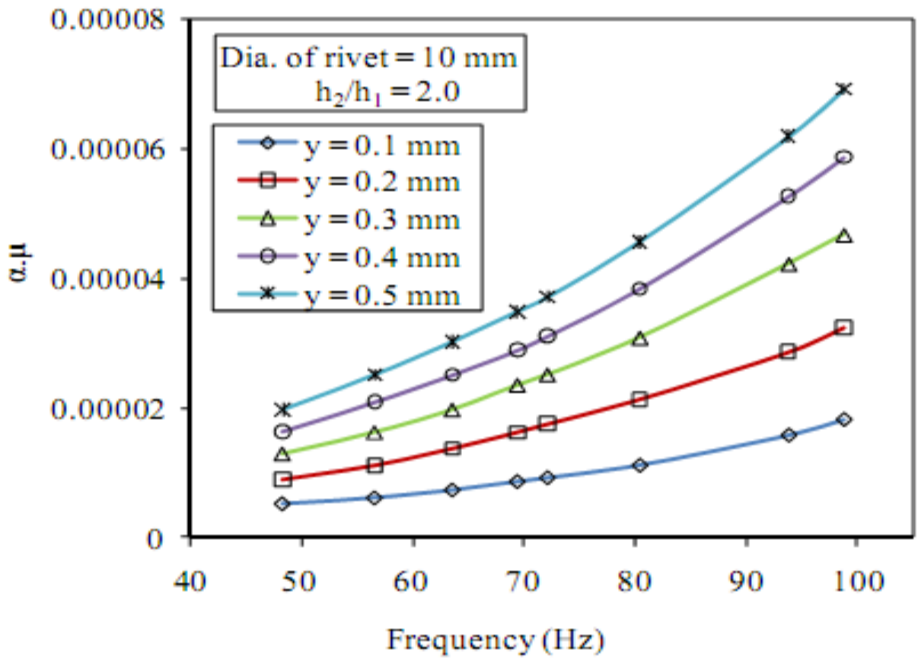

Figure 31: Variation of α.μ with frequency of vibration for mild steel specimens with beam thickness ratio 2.0 at different initial amplitudes of excitation (y)

5.2 Discussion:

From the experimental results, the following salient points have been observed and discussed in details as given below.

- Damping ratio of layered and jointed structures decreases with increase in the initial amplitude of excitation. With an increase in initial amplitude of excitation the input strain energy into the system is increased. Also with the increase in initial amplitude of excitation the energy loss also increased. However, the rate of loss of energy is less compared to input strain energy thereby resulting in lower damping.
- Damping ratio of layered and jointed structures increases with decreases in the distance between riveted joints and maintain uniformity throughout the contacting surface for a particular spacing of the connecting rivets which has been found to be 2,3539 times the diameter of the rivet.
- Damping ratio of layered and jointed structures increases with an increase in the length. The increase in length results in an increased interface length thereby resulting in an increased area for energy dissipation of the structures. Thus increased contact area results in more energy dissipation.

Chapter 6

6 Conclusions

The knowledge of estimating and enhancing the damping capacity in fabricated structures jointed with rivets is very essential for the noise and vibration control engineers. The following important conclusions have been derived from the present investigation for suppressing the undesirable effects of vibration and noise in beams with riveted joints. The effect of the influencing parameters on the damping capacity of layered and jointed riveted structures is enumerated from the theoretical and experimental results as detailed below.

1. ***Effect of interface pressure distribution***:- It is established that the pressure distribution varies depending on the thickness ratios. It is found from the theory that the interface pressure increases with the decrease in thickness ratio and is maximum for thickness ratio of 1.0 for which the average pressure at the interfaces is also high. This signifies that the normal force and hence the energy dissipation (damping) is more in case of lower thickness ratio. Therefore, the greatest possible damping can be achieved in case of jointed structures using components of equal thickness.
2. ***Effect of dynamic slip ratio***:-the logarithmic decrement increases with increase in dynamic slip ratio.
3. ***Effect of coefficient of friction***:- The friction force in a joint arises from the shearing action between the parts and is governed by the preload on the rivet and friction coefficient. As discussed, both dynamic slip ratio (α) and coefficient of friction (μ) are interdependent and show complicated behavior under dynamic condition. The energy dissipation is a function their product ($\alpha.\mu$).

4. ***Effect of beam thickness ratio***:- The combined effect of the observation, results in the increase of the logarithmic decrement with the lower thickness ratio. Therefore, the greatest possible damping can be achieved in case of jointed structures with lower thickness ratio, i.e., using components of equal thickness.
5. ***Effect of length of specimen***:- There is a reduction in the static bending stiffness with an increase in the length of the specimen so that the strain energy introduced into the system is decreased. As the longer specimens accommodate more number of rivets, there will be an increase in the overall dynamic slip, thereby causing more energy loss. Moreover, the energy dissipation is enhanced as the contact area of the interface undergoing micro-slip increases with the specimen length. The net effect of all these improves the damping with an increase in the length.
6. ***Effect of amplitude of vibration***:- The increase in the amplitude of vibration results in more input strain energy to the system .It is found from the results that the energy loss occurs at a slower rate compared to the input strain energy. and hence as the amplitudes of excitation increases, there is a decrease the logarithmic decrement.
7. ***Effect of diameter of rivet***:- The use of rivets of larger diameter increases the preload on the rivets, thereby increasing the normal force and the energy loss at the interfaces.
8. ***Effect of number of layers***:- As discussed earlier, the thickness ratio of 1.0 yields maximum damping of jointed structures. This damping will further increase with the use of more number of layers compared to the solid beam of same overall thickness due to more friction interfaces which produces higher energy loss at the interfaces.

6.1 Summary of the desired properties in a structure

The following important design guidelines have been derived from the present investigation for suppressing the undesirable effects of vibration and noise in beams with riveted joints.

- Increasing the number of layers in a beam
- Increasing the diameter of the rivets
- Increasing the fixed beam span
- Decreasing the thickness ratio of the beam with constant overall thickness
- Decreasing the thickness of the beam
- Decreasing the initial amplitude of excitation

6.2 Possibility of future work:

In the present investigation, the mechanism of damping and the various parameters affecting the damping capacity of layered and jointed riveted structures have been presented in detail to enable the engineers to design the structures depending upon their damping capacity in real applications.

- Timoshenko beam theory can be used for analysis instead of Euler-Bernoulli beam theory.
- Higher modes of vibration can be included in the analysis.
- The problem can be studied considering the nonlinearity effects of slip, friction and joint properties.
- Frequency domain analysis can be employed.
- The analysis can be extended to other boundary conditions such as continuous, fixed-supported, supported-supported, etc.
- The analysis can be made for layered and jointed beams of dissimilar materials and composites.

References

1. Cocliardt, A.W., *High Damping Alloy and Members Prepared Therefrom*. 1958, Google Patents.

2. Bert, C.W., *Material damping: An introductory review of mathematic measures and experimental technique.* Journal of Sound and Vibration, 1973. **29**(2): p. 129-153.

3. Lazan, B.J., *Damping of materials and members in structural mechanics*. Vol. 214. 1968: Pergamon press London.

4. De Silva, C.W., *Vibration damping, control, and design*. 2007: CRC Press.

5. De Silva, C.W., *Vibration: fundamentals and practice*. Vol. 978. 2007: CRC.

6. Damisa, O., et al., *'Static analysis of slip damping with clamped laminated beams.* European Journal of Scientific Research, ISSN, 2005: p. 455-476.

7. Pian, T., *Structural damping of a simple built-up beam with riveted joints in bending.* ASME Journal of Applied Mechanics, 1957. **24**: p. 35-38.

8. Chopra, A.K. and F. Naeim, *Dynamics of structures—theory and applications to earthquake engineering.* Earthquake Spectra, 2007. **23**: p. 491.

9. Chen, J., S. Hsieh, and A. Lee, *The failure of threaded fasteners due to vibration.* Proceedings of the Institution of Mechanical Engineers, Part C: Journal of Mechanical Engineering Science, 2005. **219**(3): p. 299.

10. Beards, C., *The damping of structural vibration by controlled interfacial slip in joints.* Journal of Vibration, Acoustics, Stress, and Reliability in Design, 1983. **105**: p. 369-372.

11. Ungar, E., *The status of engineering knowledge concerning the damping of built-up structures.* Journal of Sound and Vibration, 1973. **26**(1): p. 141-154.

12. Beards, C., *Damping in structural joints.* Shock and Vibration Inform. Center The Shock and Vibration Digest, 1979. **11**(9).

13. Ibrahim, R., et al., *Experimental investigation of friction-induced noise in disc brake systems.* International Journal of Vehicle Design, 2000. **23**(3): p. 218-240.

14. Gaul, L. and R. Nitsche, *Friction control for vibration suppression.* Mechanical Systems and Signal Processing, 2000. **14**(2): p. 139-150.

15. Hoffmann, N., et al., *A minimal model for studying properties of the mode-coupling type instability in friction induced oscillations.* Mechanics Research Communications, 2002. **29**(4): p. 197-205.

16. Donnelly Jr, R.P. and R.L. Hinrichsen, *The effect of energy dissipation due to friction at the joint of a simple beam structure.* Mathematical and Computer Modelling, 1988. **11**: p. 1022-1027.

17. Groper, M., *Microslip and macroslip in bolted joints.* Experimental Mechanics, 1985. **25**(2): p. 171-174.

18. Beards, C. and J. Williams, *The damping of structural vibration by rotational slip in joints.* Journal of Sound and Vibration, 1977. **53**(3): p. 333-340.

19. Goodman, L., *A review of progress in analysis of interfacial slip damping*. 1959.

20. MASUKO, M., Y. ITO, and K. YOSHIDA, *Theoretical analysis for a damping ratio of a jointed cantibeam.* Bulletin of JSME, 1973. **16**(99): p. 1421-1432.

21. NISHIWAKI, N., et al., *A Study on Damping Capacity of a Jointed Cantilever Beam: 1st Report; Experimental Results.* Bulletin of JSME, 1978. **21**(153): p. 524-531.

22. NISHIWAKI, N., et al., *A Study on Damping Capacity of a Jointed Cantilever Beam: 2nd Report, Comparison between Theoretical and Experimental Values.* Bulletin of JSME, 1980. **23**(177): p. 469-475.

23. Olofsson, U. and L. Hagman, *A model for micro-slip between flat surfaces based on deformation of ellipsoidal elastic bodies.* Tribology international, 1997. **30**(8): p. 599-603.

24. Ying, R., *The analysis and identification of friction joint parameters in the dynamic response of structures.* Department of Mechanical Engineering: Imperial College Thesis (Mar. 1992), 1992: p. 1-267.

25. Thomson, W., *Theory of vibration with applications*. 2004: Taylor & Francis.

26. Den Hartog, J., *Forced vibrations with combined Coulomb and viscous friction.* Trans. ASME, 1931. **53**(APM-53-9): p. 107-115.

27. Goodman, L. and J. Klumpf, *Analysis of slip damping with reference to turbine blade vibration.* J. Appi. Mech, 1956. **23**(3): p. 421-429.

28. Motosh, N., *Stress distribution in joints of bolted or riveted connections*. 1974.

29. Sidorov, O., *Change of the damping of vibrations in the course of operation in dependence on the parameters of bolted joints.* Strength of Materials, 1982. **14**(5): p. 671-675.

30. El-Zahry, R., *Investigation of the vibration behavior of pre-loaded bolted joints.* Dirasat-Eng. Technology, 1985. **12**: p. 201-223.

31. Marshall, M., R. Lewis, and R. Dwyer-Joyce, *Characterisation of contact pressure distribution in bolted joints.* Strain, 2006. **42**(1): p. 31-43.

32. KOBAYASHI, T. and T. MATSUBAYASHI, *Considerations on the improvement of the stiffness of bolted joints in machine tools.* Bulletin of JSME, 1986. **29**(257): p. 3934-3937.

33. Damisa, O., et al., *Dynamic analysis of slip damping in clamped layered beams with non-uniform pressure distribution at the interface.* Journal of Sound and Vibration, 2008. **309**(3-5): p. 349-374.

34. Shin, Y., J. Iverson, and K. Kim, *Experimental studies on damping characteristics of bolted joints for plates and shells.* Journal of pressure vessel technology, 1991. **113**: p. 402.

35. Gould, H.H. and B. Mikic, *Areas of contact and pressure distribution in bolted joints*. 1970, Cambridge, Mass.: MIT Engineering Projects Laboratory,[1970].

36. Ziada, H. and E.L.L. ABD, *Load, pressure distribution and contact area in bolted joints.* Institution of Engineers(India), Journal, Mechanical Engineering Division, 1980. **61**: p. 93-100.

37. Nanda, B. and A. Behera, *Study on damping in layered and jointed structures with uniform pressure distribution at the interfaces.* Journal of Sound and Vibration, 1999. **226**(4): p. 607-624.

38. MINAKUCHI, Y., T. KOIZUMI, and T. SHIBUYA, *Contact pressure measurement by means of ultrasonic waves using angle probes.* Bulletin of the JSME, 1985. **28**(243): p. 1859-1863.